UNIVERSITY OF NAPOLI FEDERICO II

Doctorate School in Molecular Medicine

Doctorate Program in
Genetics and Molecular Medicine
Coordinator: Prof. Lucio Nitsch
XXVI Cycle

New Therapeutic Perspective in CCDC6 Deficient Lung Cancer Cells

CANDIDATE Francesco Morra

Napoli 2014

New Therapeutic Perspective in CCDC6 Deficient Lung Cancer Cells

TABLE OF CONTENTS

LIST OF PUBBLICATIONS

This dissertation is based upon the following publications:

1) Staibano S, Ilardi G, Leone V, Luise C, Merolla F, Esposito F**, Morra F**, Siano M, Franco R, Fusco A, Chieffi P, Celetti A.
"Critical role of CCDC6 in the neoplastic growth of testicular germ cell tumor", BMC Cancer. 2013;13: 433.

2) **Francesco Morra***, Chiara Luise*, Roberta Visconti, Stefania Staibano, Francesco Merolla, Gianluca Guggino, Gennaro Ilardi, Renato Franco, Roberto Monaco, Simona Paladino, Daniela Sarnataro, Roberto Pacelli, Guglielmo Monaco, Aniello Cerrato, Spiros Linardopoulos, Mark T Muller and Angela Celetti.
"New therapeutic perspectives in CCDC6 deficient lung cancer cells", submitted for publication (* co-authorship).

3) Chiara Luise, Francesco Merolla, **Francesco Morra**, David Colecchia, Mario Chiariello, Vincenza Leone, Hiro Inuzuka, and Angela Celetti.
"Impairments of the CCDC6 protein oscillation during cell cycle progression contributes to neoplastic transformation", submitted for publication.

4)**Francesco Morra**, Chiara Luise, Stefania Staibano, Roberta Visconti, Gennaro Ilardi, Roberto Monaco, Gianluca Guggino, Aniello Cerrato, Mark T Muller and Angela Celetti.
"Epigenetic mechanisms are involved in the loss of the CCDC6 protein expression in NSCLC suggesting novel therapeutic options", submitted for publication.

LIST OF ABBREVIATIONS

ADC	Adenocarcinoma
ATM	Ataxia–telangiectasia mutated
ATR	ATM and Rad3 – related kinase
BER	Base excision repair
BLM	Bloom helicase
CHK1 and CHK2	Checkpoint kinase 1 and Checkpoint kinase 2
aCML	Atypical chronic myelogeneous leukeamia
DFS	Disease Free Survival
DDR	DNA damage response
DNAPK	DNA–dependent protein kinase
DSBs	Double strand breaks
EXO1	Exonuclease 1
H&E	Haematoxylin and eosin
HR	Homologous recombination
LCC	Large cell cancer
NHEJ	Non Homologous End Joining
NSCLC	Non-small cell lung cancer
ORF	Open reading frame
OS	Overall survival
PARP	Poly (ADP–ribose) polymerase
PCNA	Proliferating cell nuclear antigen
PFS	Progression free survival
PP4	Protein Phosphatase 4
SCC	Squamous cell carcinoma
SCLC	Small cell lung cancer
SSB	Single–strand breaks
TMA	Tissue Micro-Array

ABSTRACT

Non-small cell lung cancer (NSCLC) is the main cause of cancer-related deaths worldwide and new therapeutic approaches for NSCLC are urgently needed.

The role of CCDC6 in cancer induction and progression still remains largely unexplored, despite its emerging role as a tumour suppressor and its involvement in apoptosis and DNA damage response.

In this study we have characterized a panel of nine NSC lung cancer cell lines for CCDC6 expression in order to evaluate their response to conventional treatments. In the NCI-H460 cells, a weak response to DNA damage and a low number of Rad51 positive foci are associated to low levels of the CCDC6 protein. Moreover, CCDC6 deficient lung cancer cells show defects in DNA repair via homologous recombination.

The CCDC6 attenuation while conferring resistance to cisplatinum sensitizes these cells to the small molecule inhibitors of PARP1/2, such as olaparib. The combination of the two drugs is more effective than each agent individually, according to the combination index (CI < 1). Stable silencing of CCDC6 in the profoundly olaparib-resistant H1975 lung adenocarcinoma cell line increases sensitivity to olaparib alone and in combination with cisplatin, showing the relationship between CCDC6 and PARP1/2 inhibitor sensitivity.

Besides the low penetrance of CCDC6 somatic mutations or the CCDC6-RET rearrangements, TMA immunostaining for CCDC6 revealed a low expression in about 30% of the NSCL tumours analyzed (45 out of 138). Compared to the stroma, the weak CCDC6 protein staining significantly correlated with the presence of lymph node metastasis (chi-squared test: $p \leq 0{,}02$). Moreover, the CCDC6 low phenotype was negatively correlated to the Disease Free Survival ($p \leq 0.01$) and the Overall Survival ($p \leq 0.05$).

We believe that the inclusion of CCDC6 in NSCLC clinical studies should provide an additional prognostic biomarker for the overall survival (OS) with also a predictive value for the resistance to conventional treatments in NSCLC patients.

CHAPTER 1–INTRODUCTION

1.1 Lung Cancer

Lung cancer is the leading cause of cancer deaths world-wide for men and women. The population segment most likely to develop lung cancer is people aged over 50, with a history of smoking (Jemal et al. 2008). Eastern Europe has the highest lung cancer mortality among men, while northern Europe and the US have the highest mortality for both men and women.

The most common cause of lung cancer is long-term exposure to tobacco smoke, which causes 80–90% of lung cancers. Nonsmokers account for 10–15% of lung cancer cases (Thun et al. 2008), often attributed to genetic factors combined to environmental dangers such as air pollution and radon gas.

Epithelial lung cancers are generally divided into two histopathological groups, the small cell lung cancer (SCLC), including the 15% of lung cancers and the non-small cell lung cancer (NSCLC), which account for approximately 85% of all lung cancers (Walker S. 2008). The classification is also based on different genetic variations, since EGFR (10%), K-Ras (20–30%) and p16ink4 (50%) mutations have been reported in NSCLC, whereas Rb (90%) and p14arf (65%) mutations are recurrent in SCLC (Ye et al. 2009; Jonson et al. 2012).

NSCLC is the most common lung cancer and is among the main cause of death. Despite advances in early detection and standard treatment, NSCLC is often diagnosed at an advanced, metastatic stage and less than 15% of patients survive 5 years beyond diagnosis (Jemal et al. 2009). The median overall survival in the metastatic setting is only 10–12 months, despite aggressive treatments (Minna and Schillerer 2008).

NSCLC is further subdivided into adenocarcinoma (ADC), squamous cell carcinoma (SCC), and large cell cancer (LCC).

Chemotherapy is recognized as an important component of treatment for all stages of the disease, including patients with completely resected early stage disease, who benefit, with improved survival rates, when adjuvant platinum–based chemotherapy is given (Chang A. 2011)

1.2 Molecular basis of NSCLC and therapeutic approaches

The recent advances in genome analysis have identified a number of genetic alterations in NSCLC that could be therapeutically exploited as predictive biomarkers for guiding treatment decision and customizing therapy eventually improving patient outcomes.

In NSCLC the expression of a number of tumor suppressor genes is lost, through a variety of mechanism, including deletion, mutations, and hypermetilation.

For example the expression of the PTEN protein is often lost or reduced while the gene is rarely mutated (Sos et al. 2009). Driver mutations in oncogenes like EGFR, HER2, KRAS, ALK, BRAF, PIK3CA, AKT1, ROS1, NRAS and MAP2K1 have been detected in NSCLC resulting in constitutively active mutant signaling proteins.

Interestingly, never smokers patients harbour mutations in either EGFR and HER2 or fusions involving ALK and ROS1. Remarkably, these driver mutations are associated with differential sensitivity to various targeted therapies. For example, lung tumours harbouring specific driver mutations in the kinase domain of EGFR are sensitive to epidermal growth factor receptor tyrosine kinase inhibitors (TKIs), gefitinib and erlotinib, but are resistant to crizotinib, the anaplastic lymphoma receptor tyrosine kinase (ALK) inhibitor. Conversely, NSCLCs with oncogenic ALK or c-Ros oncogene 1 receptor tyrosine kinase (ROS1) fusions are sensitive to crizotinib and resistant to erlotinib and gefitinib (Pao and Hutchinson 2012).

Recently, in lung adenocarcinoma, novel gene fusions involving the RET protooncogene, which rearranges either with the kinesin family member 5B (KIF5B-RET) or with the Coiled-Coil Containing 6 protein (CCDC6–RET) have been identified (Takeuchi et al. 2012).

Results from preclinical studies and the mutual exclusivity of these novel RET gene fusions with the mutations in EGFR, KRAS and ALK genes, suggest that they are novel driver oncogenes in NSC lung adenocarcinoma and that new therapeutic approaches could be envisaged by the use of the multi-tyrosine kinase inhibitors against RET tyrosine kinase (Okamoto et al. 2013).

Unfortunately, the vast majority of NSCLC do not carry the described alterations and therefore the management of patients with lung cancer continues to pose a considerable challenge to today's oncologist.

As lung cancer cells acquire resistance to the chemotherapeutic agents, future management may lie in individualizing therapy through the careful selection of appropriate agents based on the likelihood of response and the development of resistance.

Platinum salts are the corner stone of NSCLC treatment, exerting their antineoplastic effect through direct binding to DNA resulting in cross-linking and ultimately apoptotic cell death. Unfortunately, their administration is limited because of cumulative haemato– and neuro-toxicities and by drug resistance. In recent studies on NSCLC patients, extreme or intermediate resistance to carboplatin was documented in 68% of samples and cisplatin resistance was documented in 63% of samples (Chang A. 2011).

Several mechanisms have been proposed to account for resistance to platinum agents including de-toxification, intracellular accumulation, and increased DNA repair capacity. Moreover, enhanced DNA repair capacity has been found to be associated also to radiotherapy resistance and poor survival in NSCLC patients. Over the past few decades, trials have evaluated the benefits of double chemotherapy by combination of cisplatin with other non platinum drugs.

The Poly (ADP–ribose) polymerase (PARP) inhibitor is one of the most promising new therapeutic approaches to NSCLC, either as a single agent or in combination with DNA-damaging agents like cisplatinum.

PARP1 is an abundant nuclear protein that has been specifically shown to bind DNA strand breaks formed by ionizing radiation or chemical DNA damaging agents, to facilitate the DNA repair (Satoh et al. 1993). PARP2 although less abundant, contribute to 5%-10% of the total PARP activity. The rapid binding of PARP1 to DNA strand breaks is critical for the resealing of DNA single–strand breaks (SSBs) during base excision repair (BER) and for the repair of topoisomerase I cleavage complexes (Murai et al. 2012).

When PARP is inhibited, SSBs degenerate to more lethal double strand breaks (DSBs) that, in absence of repair by homologous recombination (HR), can induce cell apoptosis. Therefore cells that are deficient in HR are highly susceptible to PARP–inhibitors in combination with platinum salts.

This finding has been clinically validated in breast cancer harboring genetic alterations in genes involved in homologous recombination, like BRCA1 and BRCA2 (Figure 1).

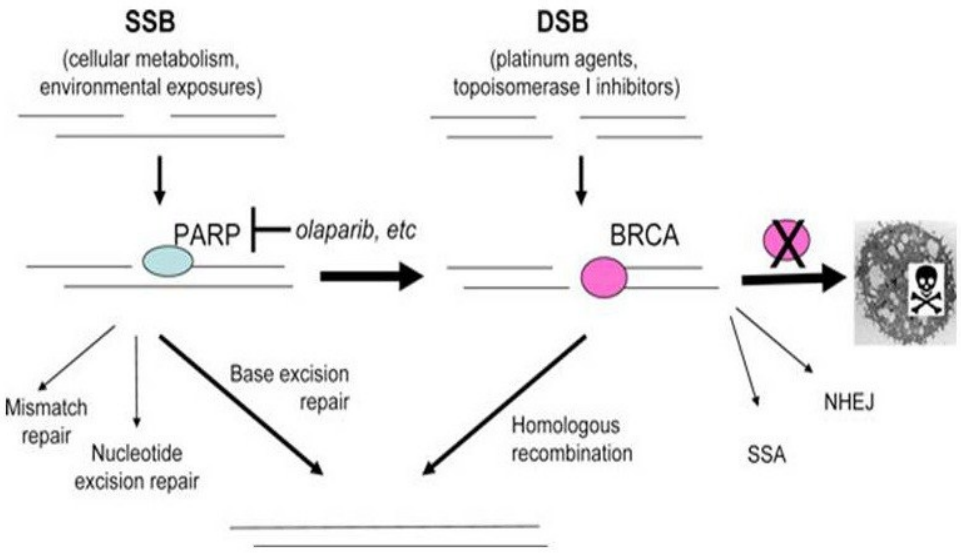

Fig.1: Mechanism of sensitivity to PARP inhibition in BRCA-deficient cells. Cells acquire DNA damage through environmental exposures or chemotherapy agents. Repair of single-strand breaks relies on PARP; repair of double-strand breaks depends on BRCA. With PARP inhibition, single-strand breaks progress to double-strand breaks. In the absence of functional BRCA, the accumulation of double-strand breaks leads to cell apoptosis or to error prone repair pathway.

Also in patients with sporadic high-grade serous ovarian cancer, PARP inhibitors efficacy reflects the high prevalence of dysfunction in key genes of HR pathway (Loveday et al. 2011).

Many other sporadic cancers have underlying defects in DNA repair pathway that could be targeted with PARP inhibitors, such as NSC lung tumours with low protein levels of ERCC1 (Postel-Vinay et al. 2013) and PTEN deficient NSCL tumours (Minami et al. 2012). Indeed, inhibiting PARP-1 activity has been established as an effective means of sensitizing tumours cells to platinum salts or other DNA-damaging agents.

1.3 PARP inhibitors in clinical use

A number of PARP inhibitors are under clinical development: rucaparib, iniparib (BSI-201), olaparib (AZD-2281; oral), veliparib (ABT-888; oral), niriparib (MK-4827), BMN-673, CEP-9722 (oral) and E7016 (GPI 21016, oral) (Kummar et al. 2012).

Olaparib has demonstrated single agent activity in women with BRCA1 or BRCA2 germline mutations with an advanced metastatic breast cancer resistant to conventional chemotherapy (Tutt et al. 2010). Over 40% of response rate has been reported in ovarian cancer patients carrying germline BRCA mutations and a platinum sensitive disease (Fong et al. 2010).

Impairments of HR pathways suggest the possibility of further treatment by the use of small molecule inhibitors of Parp1/2 in additional tumours. Similar abnormalities in DNA repair pathways have also been reported in primary peritoneal cancers patients, and in patients with Triple Negative Breast Cancer (TNB), representing the basis for recent clinical trials that have been exploring the use of PARP inhibitors in such patients population (Gelmon et al. 2011). Despite the use of PARP inhibitor in a number of clinical trials, the degree and duration of inhibition required for optimal clinical benefit has yet to be established (Kummar et al. 2009).

In NSCLC, clinical trials including PARP inhibitors as single agents or in combination with other chemotherapeutic drugs have been reported (Sandhu et al. 2013). Veliparib is currently included in a phase II multicenter first-line randomized trial in patient with NSCLC, associated or not associated with carboplatin/paclitaxel. The trial primary endpoint is the progression free survival (PFS) (Spigel 2012).

1.4 DNA damage response

Maintenance of genomic integrity is an essential part of cellular physiology. Insults that induce DNA breaks must be repaired in order to prevent the propagation of mutations that can contribute to malignant transformation. DNA damage is continuously generated by a variety of mechanism including cell metabolism, exogenous genotoxic agents and the collapse of replication forks. Amongst the many types of DNA

lesions, DNA double strand breaks (DSBs) are especially lethal if left unrepaired (Sonoda et al. 2006).

The process by which cells repair DNA damage and coordinate the repair with the cell cycle, are known as DNA damage response (DDR) (Zhou and Elledge 2000). DNA damage is recognized by sensor proteins that initiate the activation of the DDR pathway. The sensors include two key protein complexes: Mre11–Rad50–Nbs1 (MRN) and Rad9–Rad1–Hus1 (9-1-1), that localize on the regions of the DSBs or on the regions of replication stress and single strand breaks (Lee and Paull 2007).

Focusing on the MRN complex: Mre11 is a protein with DNA exonuclease and endonuclease activities; Rad50 keep the broken ends of the DNA together while Nbs1 recruit signal transducing kinases to the break site and mediates the DDR signal. The structure of 9-1-1 resembles the structure of the proliferating cell nuclear antigen (PCNA) sliding clamp loaded onto DNA at point of replication.

The localization of the MRN and 9-1-1 complexes to the sites of DNA damage activate the signal transducing kinases Ataxia – telangiectasia mutated (ATM), the ATM and Rad3 – related kinase(ATR), and the DNA – dependent protein kinase (DNAPK), which are member of the phosphoinositide 3-kinase related kinase family (Freeman and Monteiro 2010).

The first event is the activation of ATM by autophosphorilation at S1981 that caused dissociation from inactive dimers into active monomers (Bakkenist CJ and Kastan MB 2003); next ATM phosphorylates Nbs1 in S343. At the same time, Nbs1 and the MRN complex are required for full activation of ATM. Along similar lines, the localization of ATR to the break site and its subsequent activation is dependent upon then 9-1-1 complex, binding between ATR and ATR–interacting protein (ATRIP), and replication protein A (RPA). RPA is a protein constitute by three subunits (RPA70, RPA32, and RPA14) that coats single – strand DNA after phosphorylation by ATM, ATR and DNA-PK on T21 and S33 of RPA32 (Freeman and Monteiro 2010).

The signal transduction by ATM and ATR proceed through the effector kinases Checkpoint kinase-1 and Checkpoint kinase-2 (CHK1 and CHK2). CHK2 is activated in response to DSB through the phosphorilation of T68 by ATM and subsequent oligomerization and autophosphorilation at T383 and T387. CHK1 is active even in unperturbed cells, but is further activated through phosphorylation of

S317 and S345 by ATR, primarily in response to single stranded breaks and replication stress (Bartek J and Lukas J 2003); its major regulator is the protein Claspin (Kumagai and Dunphy 2000).

Several mediator proteins such as BRCA1, MDC1, 53BP1, and H2AX, work to coordinate the localization of various factors in the DDR, promote their activation, and regulate substrate accessibility.

The amminoacids S1387 and S1423 of BRCA1 are targets of phosphorylations by ATM and these phosphorylations are required for the intra-S and G2/M checkpoints, respectively.

MDC1 functions as molecular scaffold to mediate parts of the DDR downstream foci formation (Mohammad DH and Yaffe 2009) (Figure2).

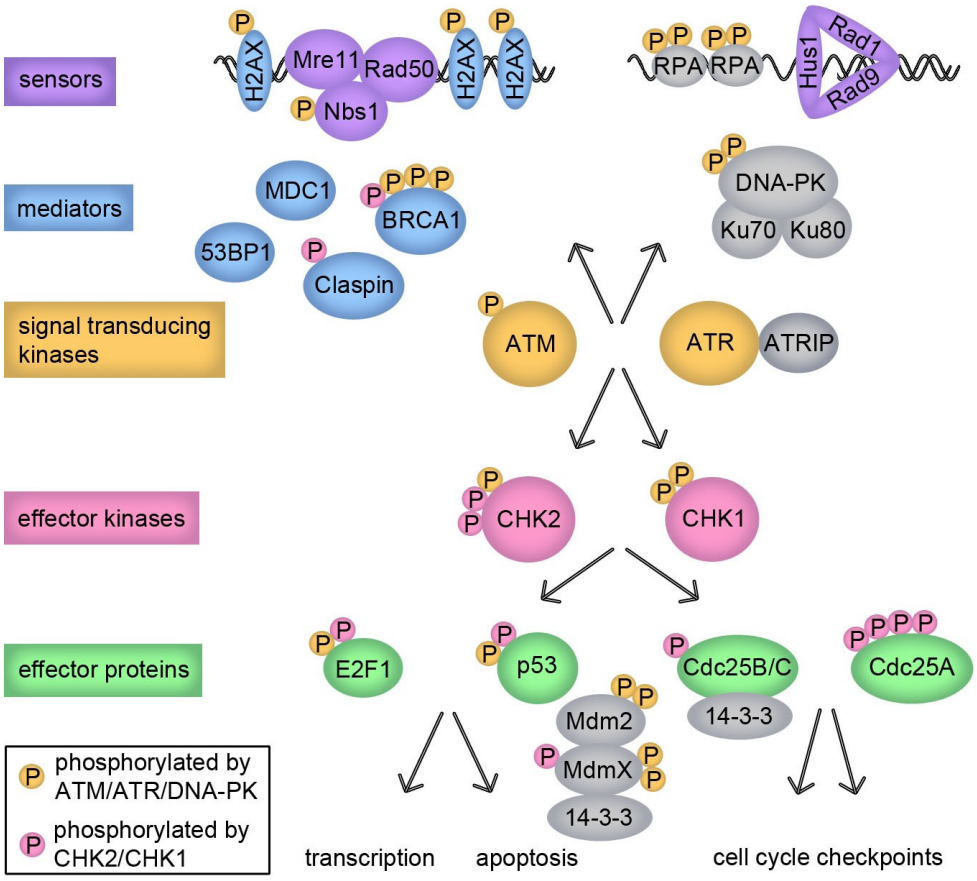

Fig. 2: A simplified view of the cellular response to DNA damage. Single and double stranded DNA breaks signal through the sensors (MRN and 9-1-1), mediators (H2AX, BRCA1, MDC1, 53BP1), signal transducing kinases (ATM, ATR), effector kinases (CHK2, CHK1), and effector proteins (E2F1, p53, Cdc25), leading to gene transcription, apoptosis, and cell cycle arrest.

There is an intricate connection between the DDR and the cell cycle; indeed, to manage the DNA damage, cells activate powerful DNA damage–induced cell cycle checkpoints that coordinate cell cycle arrest with recruitment and activation of DNA repair machinery. If the DNA damage cannot be repaired, the prolonged cell cycle arrest can lead to senescence or to apoptosis.

The overall importance of these cell cycle checkpoints in maintaining genomic integrity is highlighted by the observation that the loss, mutation, or epigenetic silencing of checkpoint genes is frequently observed in cancer (Hoeijmakers 2001).

One of the key component involved in the connection between cell cycle and DDR is the protein H2AX. H2AX is a member of the histone H2A family, one of the five families of histone that package and organize eukaryotic DNA into chromatin. The phosphorylation of H2AX (γH2AX) is among the earliest response to DNA damage, and controls the widespread accumulation of checkpoint response proteins to large chromatin regions surrounding the break sites (Rogakou et al. 1998).

H2AX is phosphorylated by ATM in the C-terminal tail on Ser139 over a region of megabases surrounding a DSB (Burma et al. 2001). In similar way, ATR phosphorylates H2AX after replicational stress.

After the repair of the DNA lesion, dephosphorilation of γH2AX, thanks to the activity of PP4 Serine/threonine phosphatase (Nakada et al. 2008), and its exclusion from chromatin regions distal to the break site are crucial passage to escape from the checkpoint and resume the cell cycle (Fernandez–Capetillo et al. 2004).

1.5 DNA Double Strand Breaks: “Two repair pathways”

The two major pathways for the repair of DNA DSBs are Non Homologous End Joining (NHEJ) and Homologous Recombination (HR). There are several types of homologous repair: gene conversion, break-induced replication and single-strand annealing. Similarly, there are also several alternative end-joining mechanisms (Haber 2000).

HR is repressed in G1, and becomes activated during S and G2 phases, while NHEJ is constitutively active throughout the cell cycle (Mao et al. 2008).

The nature of DSBs caused by replication block is quite different from that caused by ionizing radiation. DNA lesions associated with DNA replication can be readily repaired by homologous recombination

by using the other intact sister–chromatids as a template, because they are localized in close proximity.

On the other hand, ionizing radiation or genotoxic agents results in “accidental” DSB at packed chromatin structure. Moreover, such DSB could hardly interact with intact homologous sequences either in homologous chromosomes or even sister-chromatids, because after replication, extensive condensation packs replicated DNA sequences in a highly ordered chromatin structure and thereby significantly separates the two sisters. Due to the difficulty of homology search, vertebrate cells have to use NHEJ to simply re-ligate the broken ends, even though NHEJ frequently results in errors in the form of sequence deletions.

Collectively, the nature of DSBs determines the usage of DSB repair pathways; if the DSB is caused by replication blockage, usually it will be repaired by homologous recombination, whereas “accidental” DSB in packed chromosomes are frequently repaired by NHEJ (Sonoda et al. 2006).

Like most DNA repair processes, there are three enzymatic activities required for repair of DSBs by the NHEJ pathway: nucleases to remove damaged DNA, polymerases to aid in the repair, and a ligase to restore the phosphodiester backbone.

When a DSB occurs, during G0 or G1 phases, following ionizing radiation or genotoxic agents exposure, some small fragments of DNA can be lost and the Ku heterodimer (Ku70/Ku80) appears likely to be the first protein to bind the DNA ends on the break site. Ku must change conformation once it binds DNA because its interactions with other proteins such as DNA-PKcs are much stronger once the Ku-DNA complex has formed. Ku is capable of interacting with: the nuclease Artemis–DNA-PKcs, the polymerases μ and λ, and the DNA ligase IV. When Ku moves internally along the DNA filament, permits DNA-PKcs to contact the DNA end, which then activates the serine/threonine kinase activity of DNA-PKcs.

Activation of the kinase activity represents one of the simplest signal transduction systems because it permits DNA-PKcs to phosphorylate itself and Artemis. The Phosphorilated Artemis changes its confrmation and starts its 5’–or 3’-endonuclease activity.

Polymerase μ or λ can fill in the gaps synthetizing a short DNA product also in a template independent manner. The end of the process is the ligation step, accomplished by the DNA ligase IV that can ligate double strand DNA molecules with compatible ends or with blunt ends.

With this kind of repair, original nucleotide sequence has been lost at the moment of the break, and additional nucleotide lost can occur during the process, with the important consequences of not restoring the original chromosomal integrity (Lieber 2008).

In contrast to NHEJ, HR operates with slower kinetics and requires a homologous template to not only repair the DSB, but to also restore the sequence around the break.

Initial step in HR is DNA nucleolytic end resection by the MRN complex along with other accessory protein such as CtIP and the tumor suppressor protein BRCA1. An eminent role for the long range resection has the Bloom helicase (BLM), Exonuclease 1 (EXO1) and DNA2 helicase/nuclease. Thereby, terminal nucleotides in the 5' ends are removed generating long 3' single–stranded DNA (ssDNA) overhangs on both sites of the breaks. The 3'–ssDNA tails, representing the substrate for HR repair machinery, are coated and stabilized by RPA (Dueva and Iliakis 2013), and subsequently associate with Rad52 and with Rad51, a recombinase that generate nucleoprotein filament also known as nuclear foci that marks the sites of DSBs.

Rad51 plays an important role, not only in HR, but also in mitotic and meiotic recombination. The complex of Rad51 and ssDNA invades intact homologous sequences to form heteroduplexes with the contribute of Rad54 protein (Sonoda et al. 2006).

After these steps a polymerase catalyzes DNA synthesis until finally the Holliday junctions become resolved, resulting in a crossover or non-crossover product (San Filippo et al. 2008).

1.6 CCDC6 gene and its products

The CCDC6 gene (Coiled Coil Containing 6) has been identified upon its frequent rearrangement with the RET proto–oncogene in papillary thyroid carcinomas (Fusco et al. 1987; Grieco et al. 1990), and with genes other than RET in solid and not solid tumours (Drechsler et al. 2007). Recently, by using an integrated molecular– and histopathology–based screening, the fusion CCDC6-RET has been detected in lung adenocarcinoma, even at low frequency (Takeuchi et al. 2012).

The CCDC6 gene is located on the long arm of chromosome 10 (10q21), and contains 9 exons that encode a transcript of 3 Kb showing an open reading frame (ORF) of 475 aa. The CCDC6 gene promoter,

localized within 259 bp upstream of the ATG site, drives the gene expression ubiquitously in various human tissues (Tong et al. 1995).

In tumours harbouring the RET/PTC1 rearrangement, the activation of RET involves chromosomal inversion of the long arm of chromosome 10 that juxtaposes the tyrosine kinase-encoding domain of RET, mapped at 10q11.2, to the promoter and the first exon of the CCDC6 gene (Pierotti et al. 1992) (Figure 3).

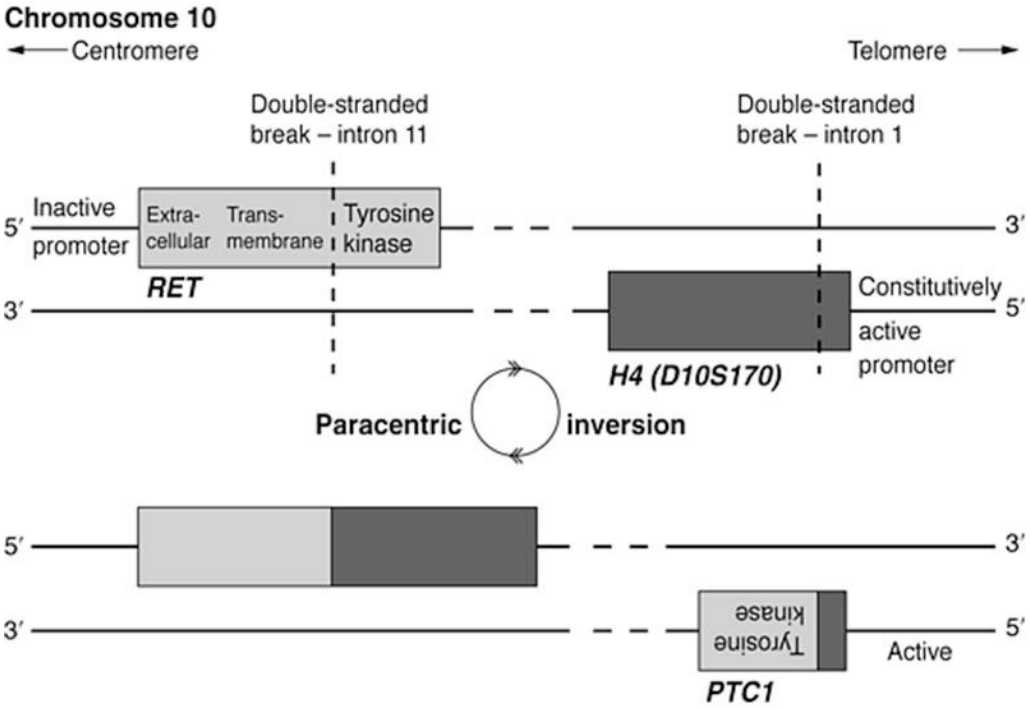

Fig. 3: Schematic view of the paracentric inversion of chromosome 10q generating the transforming sequence RET/PTC1.

Sequencing analysis of CCDC6 cDNA shows that CCDC6 has not significant homology to know genes; its predicted amino–acid (aa) sequence contains a long coiled-coil region and a putative binding domain for SH3–proteins, suggesting its possible involvement in protein–protein interactions (Grieco et al. 1994).

CCDC6 gene product shows extensive regions of alpha helices which have a high potential to adopt a coiled-coil conformation. Coiled–coils are formed by two or three alpha–helices that are strongly

amphipathic and supercoil around each other, crossing at an angle of about 20° (Lupas et al. 1991). It has been demonstrate that such region can be involved in protein dimerization or oligomerization.

The 60 amino acid fragment of the CCDC6 coiled-coil domain included in the RET/PTC1 gene product rearrangement, has been shown to be necessary for homodimerization, constitutive activation and transforming ability of the oncoprotein (Tong et al. 1997 Jhiang, 2000).

In some cases of atypical chronic myelogeneous leukaemia (aCML) the first 368 aa of CCDC6 has been found fused to the tyrosine kinase domain of the PDGFRβ. The chromosomal event is a t(5;10) translocation. In the cases of atypical CML in which the CCDC6-PDGFRβ rearrangement has been identified, the fusion product is a protein of 948 aa containing most of the coiled–coil domain of CCDC6 and the transmembrane and the tyrosine kinase domains of the PDGFRβ. The reciprocal product of the translocation has not been found (Kulkarni et al. 2000; Schwaller et al. 2001).

Moreover, CCDC6-PTEN rearrangements have also been identified in irradiated thyroid cell lines. Sequencing analysis revealed a transcript consisting of exon 1 and 2 of CCDC6 fused with exon 3 and 6 of PTEN (Puxeddu et al. 2005) (Figure 4).

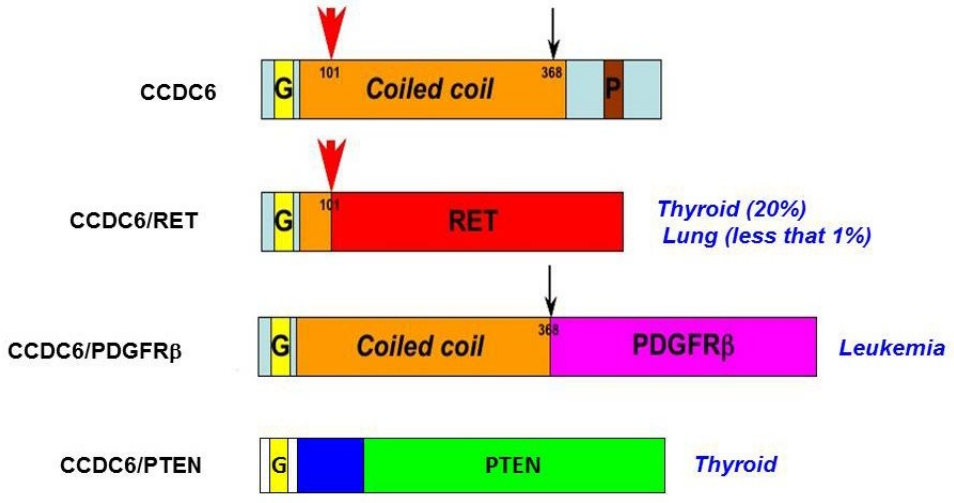

Fig.4: CCDC6 rearrangements. The red arrow shows the RET/PTC1 and the black one shows the CCDC6/PDGFRβ breakpoint.

Notably, in most cancer harbouring CCDC6 gene rearrangements, the product of the normal allele is absent or functionally inactivated by a dominant negative mechanism (Celetti et al. 2004).

CCDC6 protein is an ubiquitously expressed 65 KDa nuclear and cytosolic protein phosphorylated by ERK1/2 at serine 244 upon serum induction (Grieco et al. 1994; Celetti et al. 2004).

Overexpression of CCDC6 in cells induces apoptosis while a CCDC6 protein truncated at the carboxiterminal, such as in the fusion with different oncogenes, acts as dominant negative on nuclear localization and on the wild–type protein–induced apoptosis (Celetti et al. 2004).

Moreover, in response to DNA damage CCDC6 is phosphorylated at T434 by the ATM kinase that stabilizes the protein in the nucleus. The loss of the CCDC6 region substrate of ATM or protein deficiency determines an increase in cell survival, allows for DNA synthesis and permits cell to progress into mitosis, following the exposure to genotoxic stress (Merolla et al. 2007).

CCDC6 gene product undergoes multiple post-translational modifications such as sumoylation (Luise et al. 2012), ubiquitination (Povlsen et al. 2012), and phosphorylation (Celetti et al. 2004; Beausoleil et al. 2004; Brill et al. 2004), suggesting that CCDC6 protein activity is highly regulated.

It has been reported that CCDC6 interacts with CREB1 and inhibits its cAMP-dependent transcriptional activity (Leone et al. 2010) in a SUMO-dependent manner (Luise et al. 2012), these results support a role of CCDC6 in control of cell proliferation and sustain the hypothesis that CCDC6 acts as a tumour suppressor.

High–throughput proteomic screening predicted the interaction between CCDC6 and the catalytic subunit of Protein Phosphatase 4 (PP4c) (Ewing et al. 2007) that we have confirmed in vitro and in vivo (Merolla et al. 2012). Moreover, it has been demonstrate that cells depleted of CCDC6 have an enhanced phosphatase activity directed toward the phosphorylation of the H2AX protein in response to ionizing radiation (IR).

Loss of CCDC6 affects the DNA damage induced G2 arrest, overcoming the G2/M checkpoint. Furthermore, loss of CCDC6 affects the DSBs DNA repair mechanism in G2 increasing the levels of the error prone, Non Homologous End Joining repair pathway (Merolla et al. 2012).

In recent studies it has been also reported that the E3 ubiquitin ligase FBXW7 specifically interacts with CCDC6 driving its degradation in a proteasomal dependent manner (Zhao et al. 2012). Moreover, CCDC6 degradation is impaired in response to DNA damage.

The post translational events that regulate the phosphorylation status and the abundance of CCDC6 during the cell cycle have been also investigated in our laboratory.

Interestingly CCDC6 sporadic mutations have been reported in primary NSCL tumours (N394Y, T462A, S351Y, E227K), in ovary cancer (CCDC6 L217P, A226S/T, P442S); in gastrointestinal tumours (110*, 139*, 229*, P243S, E285, Q450*); in endometrious carcinomas (M287I); in breast cancer (CCDC6 E300D, T452M, R425W), (www.sanger.ac.uk/genetics/CGP/cosmic).

Thus, CCDC6 is an attractive candidate marker whose loss or inactivation could enhance tumour progression by impairing apoptotic response and by overcoming a DNA damage response-dependent barrier.

It has been recently reported that the loss of CCDC6 in the Testicular Germ Cell Tumours (TGCTs) aids the spermatogonial cells to benefit from a pro-survival pathway in order to evade the toxic effects of endogenous oxidants and finally promoting testicular neoplastic growth (Staibano et al. 2013).

In this dissertation we have evaluated the CCDC6 role in NSCLC.

CHAPTER 2–AIMS OF THE STUDY

The purpose of the present dissertation has been to evaluate the CCDC6 expression in a wide panel of NSCLC cell lines.

Depending on the expression levels of CCDC6 in NSCLC cell lines we have verified:

1) The formation of Rad51 foci and the DNA damage response
2) The proficiency of the homology-directed repair.
3) The response to standard treatments and to PARP1/2 inhibitors.

Next, we have assessed the CCDC6 expression in a wide range of early resected or locally advanced NSCLC primary tumours and we have investigated

4) The statistical significance of the correlation between CCDC6 immunostaining and the presence of lymph node metastasis.
5) The statistical significance of the correlation between the CCDC6 immunostaining, the Disease free survival (DFS) and the Overall survival.

Our final goal is to highlight CCDC6 as a prognostic marker for the overall survival with also a predictive value for the resistance to conventional treatments in NSCLC.

The possibility that CCDC6 could be a predictive biomarkers of sensitivity to the PARP1/2 inhibitors has been also investigated.

CHAPTER 3-MATERIALS AND METHODS

3.1 Cell Culture

Human Non Small cell lung cancer cell lines, with different genetic backgrounds (EGF-R, RAS, PKI3CA, TP53, and CDKN2A mutations) (www.sanger.ac.uk/genetics/CGP/cosmic), have been kindly obtained by Professor Giuseppe Viglietto: ADC (NCI – H1975, A549, NCI-H23, NCI-H522, NCI-H1299, NCI-Calu3, NCI-Sw1573), SCC (NCI-H292) and LCC (NCI–H460). Cells were maintained in RPMI (Gibco, Paisley, UK), supplemented with 10% fetal bovine serum, 100 U/ml of L- Glutamine and 100 U/ml of penicillin – streptomycin (Gibco, Paisley, UK).

3.2 Plasmids and Transfection

The silencing of CCDC6 were from Sigma-Aldrich, Inc. For stable transfection assays the H1975 cells were transfected with the plasmid pool (shCCDC6, NM_005436) or a pool of non-targeting vectors (shcontrol) by the Nucleofector transfection system. Lipofectamin 2000 was used accordingly to the manufacturer (Invitrogen), for transient transfection with the DR-GFP and the I-SceI plasmids. The DR-GFP reporter plasmid has been developed by M.Jasin (Pierce et al. 1999). PcDNA4ToA-CCDC6 plasmid has been transfected with FuGene HD (Promega) and it has been described elsewhere (Celetti et al. 2004).

3.3 Protein Extraction and Western Blot Analysis

Total cell extracts (TCE) were obtained by Ripa buffer (50 mM Tris–HCl pH 7.5, 150 mM NaCl, 1% Triton X-100, 0.5% Na Deoxycholate, 0.1% SDS) or Lysis buffer (20mM Tris-HCL pH7.5, 150mM NaCl, 1% Triton X-100) and a mix of protease inhibitors. Protein concentration was estimated by a modified Bradford assay (Bio-Rad). Membranes were blocked with 5% TBS-BSA proteins and incubated with the primary antibodies.

Immunoblotting and immunoprecipitation experiments were carried out according to standard procedures and visualized using the ECL chemiluminescence system (Amersham/Pharmacia Biotech).

3.4 Real Time PCR

PCR reactions were performed on RNA isolated, from cell lines and from primary tissue using RNeasy Mini Kit (Quiagen). RNA (1 μg) was reverse-transcribed using a mixture of poly-dT and random exonucleotides as primers and MuLV RT (Invitrogen). PCR reverse transcription was performed according to standard procedures (Invitrogen).

qRT-PCR analysis was performed with Syber Green (Agilent), using the follows primers annealing at CCDC6 amino-terminus: Forward GGAGAAAGAAACCCTTGCTG and Reverse TCTTCATCAGTTTGTTGACCTGA. Primers for GAPDH were used for normalization of qRT-PCR data. To calculate the relative expression levels we used the $2^{-\Delta\Delta CT}$ method.

3.5 TMA

Tissue Micro-Array (TMA) was built using the most representative areas from each single case. Tissue cylinders with a diameter of 0.3 mm were punched from morphologically representative tissue areas of each ‘donor’ tissue block and brought into one recipient paraffin block (3×2.5 cm) using a semiautomated tissue arrayer (Galileo TMA, Milan, Italy).

3.6 IHC Analysis

For light microscopy, tissues were fixed by immersion in 10% formalin and embedded in paraffin by standard procedures; 4 μm sections were stained with haematoxylin and eosin (H&E) or processed for immunohistochemistry. The sections were incubated overnight with antibodies against CCDC6, HPA-019051 (Sigma-Aldrich, Co. LLC) at 1: 200 dilution. The following controls were performed: (a) omission of the primary antibody; (b) substitution of the primary antiserum with non-

immune serum diluted 1: 500 in blocking buffer; (c) addition of the target peptide used to produce the antibody (10^{-6} M); no immunostaining was observed after any of the control procedures.

The immunohistochemical staining of CCDC6 will be evaluated semiquantitatively as the percentage of positive cells (with either nuclear or cytoplasmic localization) among the total number of cells and classified as: low staining [including 0(<5%) and +(5-25%)] and high staining [including ++(26-50%) and +++(>50%)].

3.7 Statistical Analysis

Student's T test or chi-squared test have been performed to assess the statistical significance of correlation between clinicopathologic characteristics of tumours, platinum response and CCDC6 expression. Disease free survival (DFS) and overall survival (OS) curves of the patients have been calculated using Kaplan-Meier method and analysis have been done by the log-rank test.

3.8 Immunofluorescence Staining

Cells were permeabilized 18h after exposure to 5Gy IR, in phosphate–buffered saline (PBS)–0.25% Triton X–100, and fixed with 4% PFA. After staining with primary antibodies for 1h at room temperature, cells were washed in PBS and incubated for 30 min at room temperature with secondary antibodies. Nuclei were visualized by staining with DAPI. Cells with a number of Foci between 5 and 10 were scored as positive.

3.9 Clonogenic Assay

Cell lines were plated at limiting dilutions into 6-well plates, incubated for 24 h, and then treated with different doses of olaparib or cisplatinum followed by incubation for ten days. Prior to counting colonies, cells were stained with crystal violet. A population of more than 50 cells was counted as one survived colony. The mean colony counts +/- standard errors are reported.

3.10 Sensitivity Test and Design for Drug Combination

Antiproliferative activity was determined by the CellTiter 96 AQueous One Solution assay (Promega), in term of 50% inhibitory concentration (IC50) values. Briefly, cells were plated in quintuplicate in 96-well plates at a density of 1,000-3,000 cells per well, and continuously exposed to each drug for 144h. Each assay was performed in quintuplicate and IC_{50} values were expressed as mean +/- standard deviation.

The results of the combined treatment were analysed according to the method of Chou and Talaly by using the CalcuSyn software program (Chou and, Talaly 1984). The resulting combination index (CI) is a quantitative measure of the degree of interaction between different drugs. If CI = 1, it denotes additivity; if CI > I, it denotes antagonism; and if CI < 1, it denotes synergism.

3.11 Reagents and Antibodies

Anti Rad51 (H92) Sc8349, anti-PARP (H250) Sc7150, were from Santa Cruz Biotechnology, Inc; Anti CCDC6 was from Abcam; Anti pS139_H2AX (05-636), anti Rad51 (07-1782) was from Millipore; Anti-H2AX, anti-pT68Chk1 and anti-Chk1 antibodies were from Cell Signaling Technology, Inc. The secondary antibodies were from Biorad. Alexa Fluor Secondary antibodies for immunofluorescence were from Invitrogen, Inc. Olaparib (AZD2281) was provided by Selleck Chemicals (Huston, TX, USA) and Cisplatin was from Sigma Chemical Co.

3.12 HR Transient Assays

H1975, H460, H1975ShCCDC6 and H460 CCDC6+ cells were plated in a 12 wells plate and transfected with the DR-GFP reporter alone (as negative control), together with the plasmid expressing the I-SceI. Wilde Type GFP was used as control of transfection. After 48h of transfections cells have been collected and analyzed by FACS analysis with Accury C6 Flow Cytometer.

3.13 HR Reporter Cell Assays

The HeLa HR-I reporter cells are based on a GFP gene with an artificially engineered 3 kb intron from the Pem1 gene (GFP-Pem1).

In the HR reporter, the first exon of GFP-Pem1 contains a 22 bp deletion combined with the insertion of three restriction sites, I-SceI-HindIII-I-SceI, which are used for inducing DSBs. The deletion ensures that GFP can not be reconstituted by an NHEJ event. The two I-SceI sites are in an inverted orientation, so that I-SceI digestion leaves incompatible ends. The first copy of GFP-Pem1 is followed by a promoter-less/ATG-less first exon and intron of GFP-Pem1. The intact construct is GFP-negative (Mao et al. 2008).

To create the I-Sce1 inducible cell reporter, a stable HeLa cell line containing a single integrated copy of the HR-I reporter was first selected and characterized. Two lentiviruses (pLV-TetO-HA-SceI and rtTA) were used to co-infect this stable cell line and screening was performed to identify a single clone that could be induced by Doxycycline to produce GFP+ cells in a Tet-on format.

After transient silencing for CCDC6 and induction of DSB with Doxycyclin (1µg/ml) the percentage of GFP positive cells were determined by immunofluorescence microscopy.

293AJ2 Cells bearing the stably integrated HR repair substrate DR1Bsd were silenced for CCDC6 and plated in the presence of 5µg/ml blasticidin (Invitrogen) or without antibiotic. The construct DR1Bsd consist of two tandem copies of the blasticidin resistance gene (Bsd).

The insertion of an I-SceI restriction site, which also encodes two in-frame stop codons, into the upstream copy of the blasticidin-resistance gene prevents its expression. The downstream copy of the gene is promoterless, and hence non – functional. Expression of the I-SceI enzyme induces DSB. The repair of this lesion by NHEJ will mostly leave the S1Bsd gene not-functional, whereas HR mechanism, using the 5'ΔBsd copy as a repair template, generates a functional gene and cell resistance to blasticidin (Tutt et al. 2001). After 21 days, cells were fixed and stained with crystal violet.

3.14 Tumors Samples

Patients underwent surgery at the Surgery Departments of Ospedale Cardarelli, Naples and NCI “Fondazione G. Pascale”, Naples, between 2005 and 2010. The patients age ranged between 47 and 80 years, with a mean of 63.5 years. Patients underwent radiological evaluation and were treated by surgery alone, except for patients with locally advanced tumors (T4), who received adjuvant therapy. The patients underwent a median of 48 months follow-up. After surgical resection, tissues were fixed in 10% neutral buffered formalin and embedded in paraffin blocks. Sections (4 mm thick) were stained with H&E.

Histologic grading and tumor-node–metastasis classification were done according to the recommendations of the International Union Against Cancer.

For six patients, a 10-mm-thick section was processed for dissection. Paraffin was removed by treatment with xylene for 3 hours at room temperature followed by tissue rehydratation through multiple graded ethanol solutions and distilled water. The cancerous region was identified microscopically; normal and tumor tissues were dissected with a sterile 30-gauge hypodermic needle. The collected samples (120000 cells) were placed into 1.5-mL microcentrifuge tubes and processed for RNA extraction.

CHAPTER 4-RESULTS

4.1 Low levels of CCDC6 in NSCLC impair Rad51 focus formation

In the present study we have investigated the CCDC6 expression in a wide panel of NSCLC cell lines observing that different NSC lung cells show different levels of CCDC6 protein at immunoblot (Figure 5).

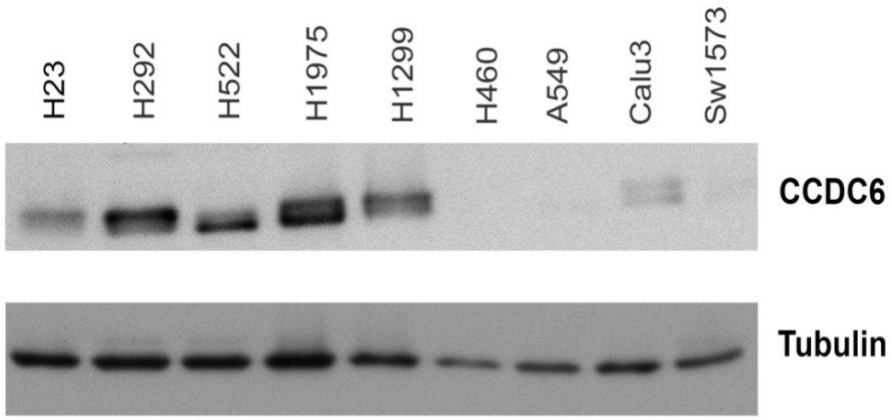

Fig.5: CCDC6 protein levels in NSCLC cell lines.

In particular, we pointed our attention on the NCI-H460 cells that exhibit barely detectable levels of CCDC6 compared to the NCI-H1975 that show a good amount of the CCDC6 protein. The real time PCR showed no significant differences in the CCDC6 mRNA expression levels between the different NSC lung cell lines suggesting that the CCDC6 protein levels in the NSC lung cancer cells were dependent on post-translational mechanisms (Figure 6).

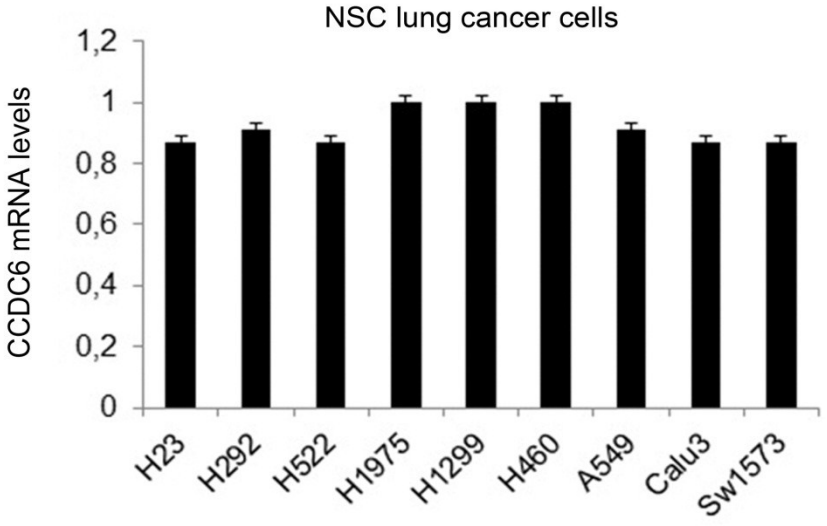

Fig. 6: CCDC6 mRNA levels in NSCLC cell lines. No variations have been found in the transcript levels.

Next, in order to investigate if in NSCLC the CCDC6 low levels could affect the DNA damage response, after 5Gy ionizing radiation exposure we investigated Chk1 activity in CCDC6-depleted lung cancer cells, compared to control. We observed that pS345 Chk1 was weakly activated 1 hour post DNA damage in CCDC6 deficient H460 cells compared to CCDC6 proficient H1975 lung cancer cells. pS139H2AX was barely activated in CCDC6 null lung cancer cells, as well.

As expected, CCDC6 protein is stabilized in H1975 cells upon IR exposure. (Figure 7).

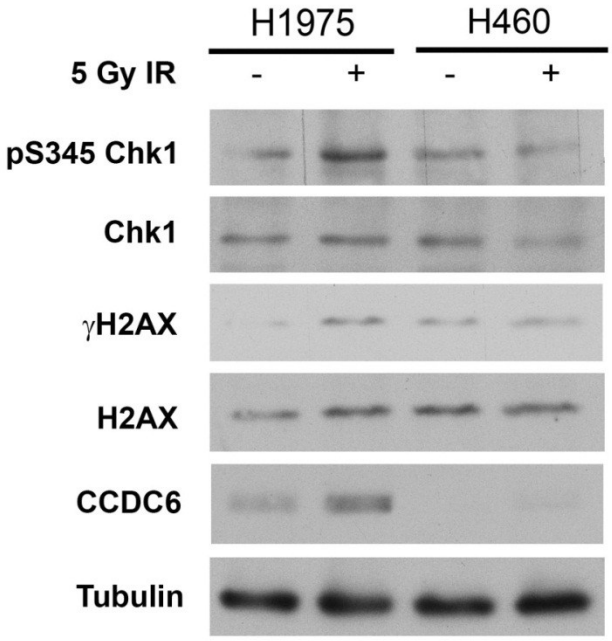

Fig. 7: CCDC6 loss in NSCLC cell lines induces a weak checkpoint and tolerance to DNA Damage.

These data suggested that loss of CCDC6 in lung cancer cells can induce a weak checkpoint response and may introduce a cellular tolerance to DNA damage, as we have previously reported in HeLa cells (Merolla F et al, 2012).

We observed that low protein levels of CCDC6 are associated to reduced protein levels of the Rad51 DNA recombinase at western blot (Figure 8).

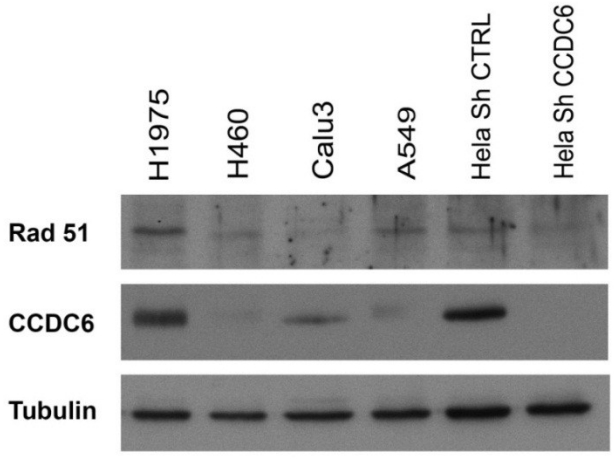

Fig. 8: Low CCDC6 protein levels in NSCLC cell lines associate to reduced Rad51 protein levels.

The Rad51 localization in DNA-damage-induced foci is likely to reflect HR repair events. The localization of these foci, after damage, most likely represents the loading of the Rad51 DNA recombinase onto damaged DNA, as an essential part of the HR process known to be controlled by other HR proteins such as BRCA1 and BRCA2.

In order to investigate the potential effect of CCDC6 on HR, we examined the formation of nuclear RAD51 foci after DNA damage in NSCLC cell lines. In the tumourigenic NSC lung cancer cells, NCI-H460, the CCDC6 attenuation causes an efficient elimination of the Rad51 foci following gamma-irradiation at 4 hours recovery, compared to the NSC NCI-H1975 cells that express good levels of the CCDC6 protein. This effect is even more evident after 18 hours recovery (Figure 9).

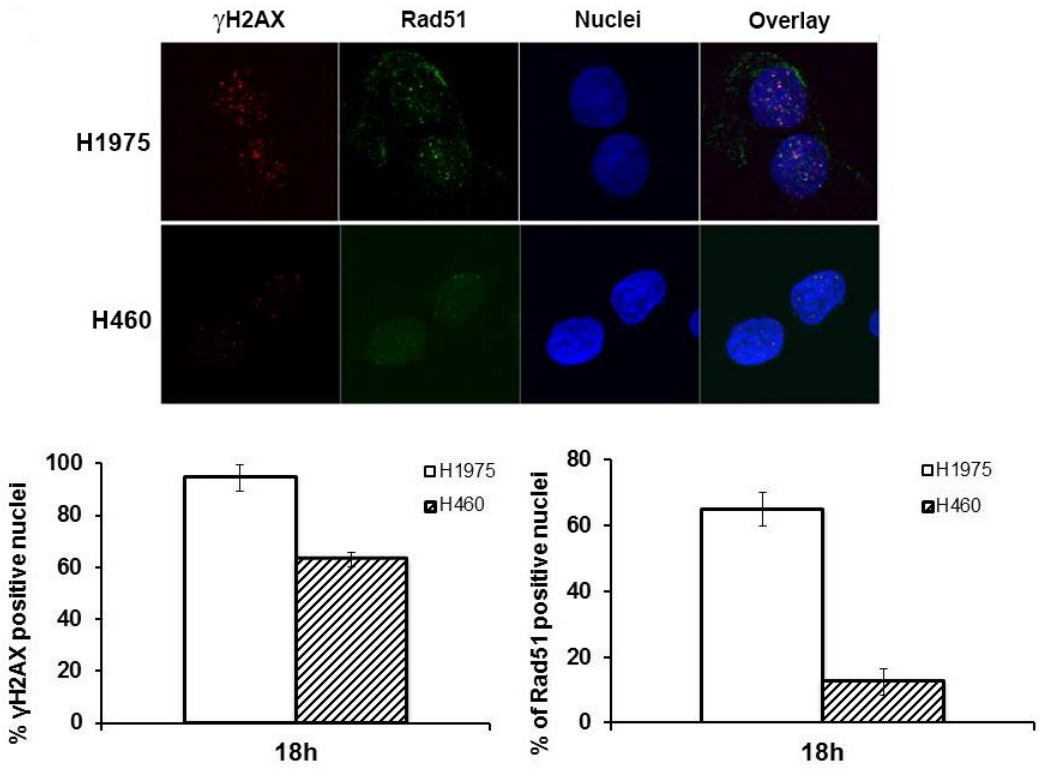

Fig. 9: CCDC6 deficiency in NSCLC cells affects Rad51 foci formation following 5Gy IR. The same result is evident also for □H2AX foci formation.

Interestingly, the stable depletion of CCDC6 in the H1975 cells (H1975 ShCCDC6 Cl4) (Figure 10), reduced the formation of Rad51 foci at different recovery times (Figure 11).

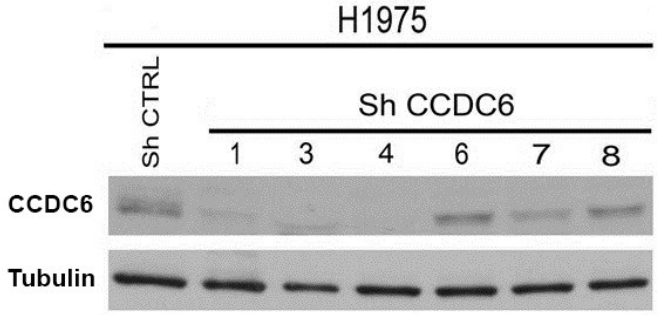

Fig. 10: Stably CCDC6 depleted NSCLC H1975 clones.

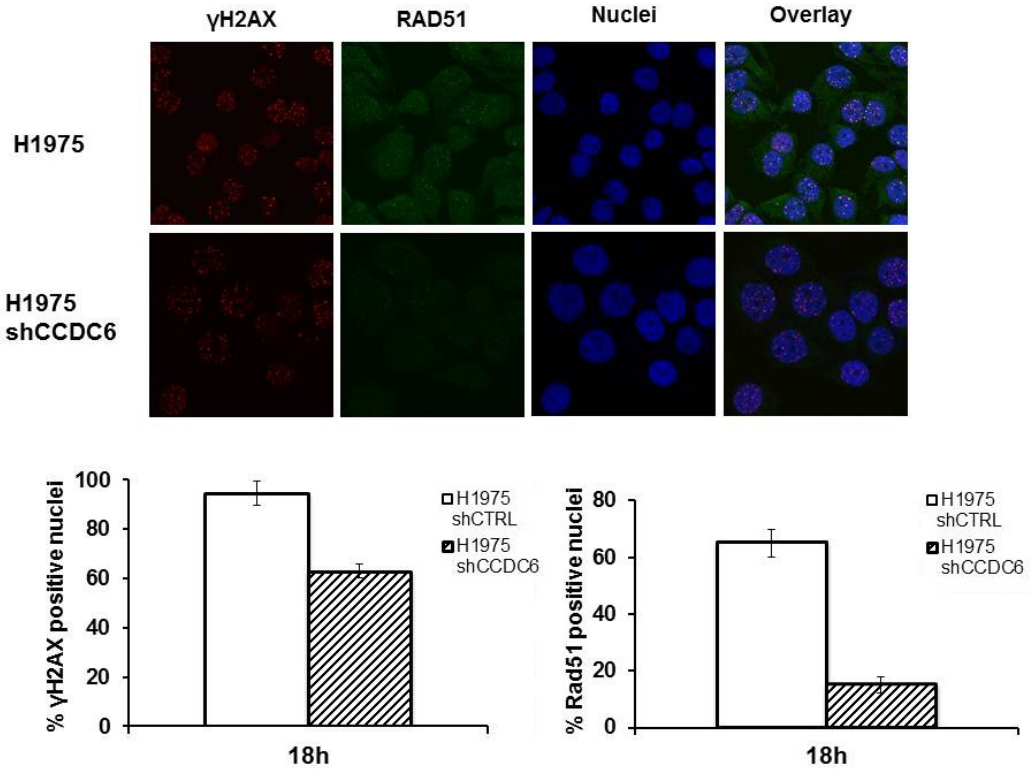

Fig.11: CCDC6 depletion in NSCLC H1975 cells affects Rad51 foci formation following 5Gy IR. The same result is evident also for γH2AX foci formation.

The observations that in naturally CCDC6-depleted NSC lung H460 cells the Rad51 focus induction was impaired suggested a potential effect of CCDC6 on HR.

In conclusion, our data suggest that CCDC6 is important for the focal accumulation of Rad51 after DNA damage from ionizing radiation.

In CCDC6 deficient NSC lung cells a few γ-H2AX foci were also appreciated (Figure 9 and 11), as we have already reported in HeLa cells (Merolla et al.2012).

4.2 CCDC6 loss inhibits homology-directed repair (HR)

In order to check the proficiency of the HR repair machinery in CCDC6 deficient cells we have pursued several approaches. First, we used a validated synthetic DSB repair substrate stably introduced into the 293 AJ2 cells (Tutt et al. 2001). This model is based on the induction of a DSB by the restriction enzyme I-SceI at a single chromosome locus (Figure 12).

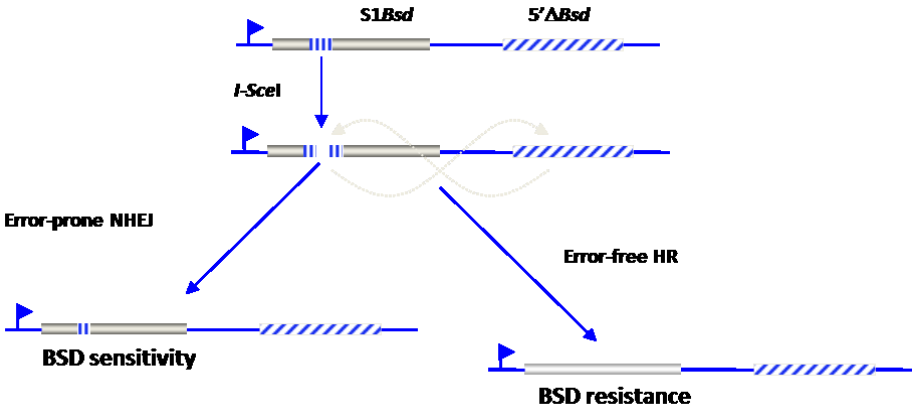

Fig. 12: Schematic representation of the mechanism of DR1Bsd reporter plasmid.

When this lesion is repaired by a homology-directed mechanism, a functional blasticidin resistance gene is generated.

We have transiently silenced CCDC6 in 293AJ2 cells (supplementary figure) and we have observed that fewer blasticidin resistant 293 cells were generated when CCDC6 was depleted, using colony formation assay to estimate blasticidin resistance. These data suggested that HR is repressed by the CCDC6 loss in this model. These results pointed to a role of CCDC6 in the control of HR. Therefore, CCDC6 activity might have a stimulating effect on DNA repair by HR (Figure 13).

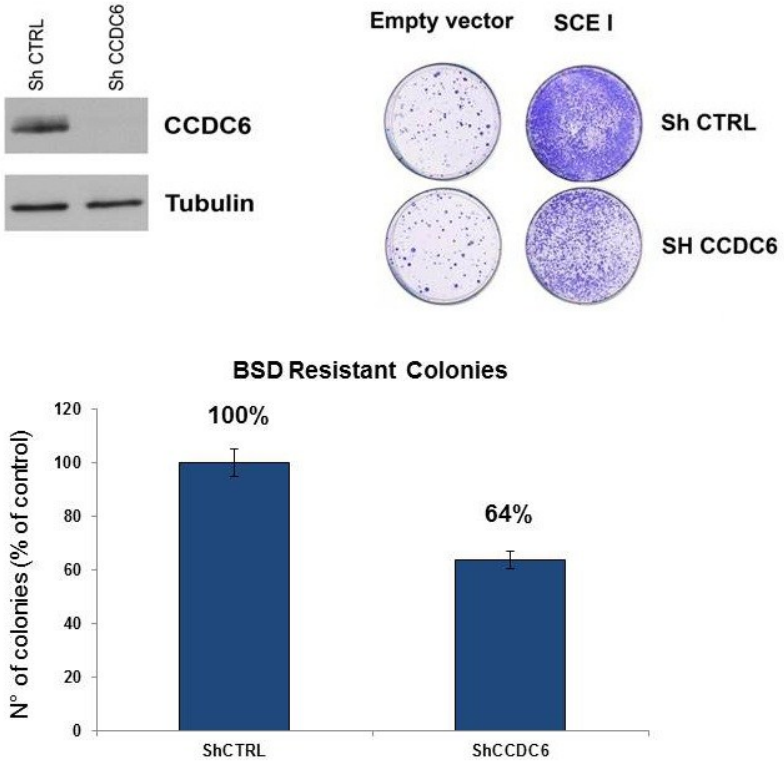

Fig. 13: CCDC6 silencing affects HR in 293AJ2 cell lines.

To examine the overall efficiency of a specific DSB repair pathway, we have also utilized a different system to quantify HR in CCDC6 proficient (shCTRL) and depleted (shCCDC6) HeLa cells. In this system, a single GFP cassette is mutated by introducing two inverted I-Sce1 homing endonuclease sites. This reporter cassette (GFP minus) was used to create a stable cell line containing a single integrated copy of the HR-I cassette (Mao et al. 2008) In the same cells, the Tet-on system was engineered to control I-SceI gene expression; therefore, in the absence of doxycycline, I-Sce1 is not present. Within a few hours after doxycycline addition, the I-Sce1 gene is robustly expressed, which introduces a unique DS DNA break in GFP followed by HR repair and the appearance of GFP positive cells, evaluated by counting them at a fluorescence microscope (Figure 14).

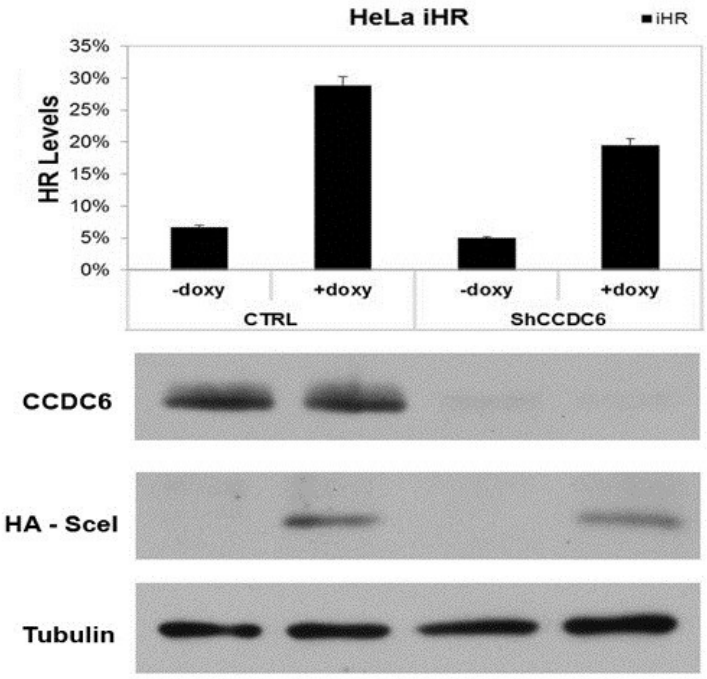

Fig. 14: CCDC6 silencing affects HR in HeLa cell lines.

The data obtained from two different assays suggested that HR, that usually is an error free pathway for DSBs repair, operates with a lower efficiency when CCDC6 is depleted in 293AJ2 cells and in Hela cells. The number of GFP+ cells reflects the overall efficiency of a specific DS repair pathway, HR. With this reporter, we observed a clear decrease in the GFP-positive cells when CCDC6 was depleted. The data obtained by two different assays suggest that HR, thought to be an error free pathway for DS break repair in animal cells, operates less effectively when CCDC6 is depleted in 293 AJ2 and HeLa cells.

Finally, in order to check the proficiency of the HR repair machinery in the NSCLC CCDC6 naturally depleted H460 and in the CCDC6 proficient H1975 cell lines, we have utilized the twin reporter DR-GFP plasmid developed by M.Jasin (Figure 15), transiently co-transfected with the plasmid encoding for the restriction enzyme I-SceI.

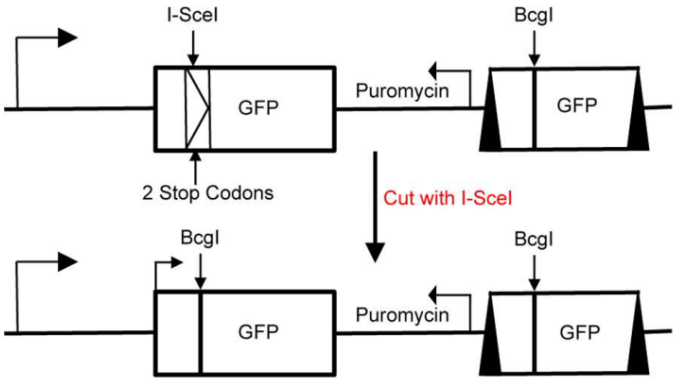

Fig. 15: Schematic representation of the DR-GFP reporter plasmid.

The reporter DR-GFP has twin cassettes (GFP-I, GFP-II) that are mutated and GFP minus. Adjacent to the cassette I there is a unique I-SceI site. The expression of I-SceI induces DSB in the 5' cassette; this lesion can be repaired by HR using as the linked donor, the GFP gene in the cassette II restoring the GFP expression (Pierce et al., 1999).

H460 and H1975 cells have been co-transfected with the plasmids containing the reporter DR-GFP and the I-SceI gene. After 48 hr of transfection, the HR frequency has been measured by FACS analysis and reported as the percentage of GFP positive cells. When I-SceI is transfected together with the reporter DR-GFP we can observe a lower number of GFP positive cells in the H460 cells compared to the H1975 cells, suggesting that low levels of the CCDC6 protein correlate with low levels of HR.

After the CCDC6 reconstitution in the H460 cells (H460-mycCCDC6), we could see an increase of GFP positive cells compared to the empty vector transfected cells (Figure 16).

The stable depletion of CCDC6 in the H1975 cells (H1975 ShCCDC6 CL1 and CL4) affects HR supporting the relationship between the low levels of the CCDC6 protein and the low levels of HR (Figure 16).

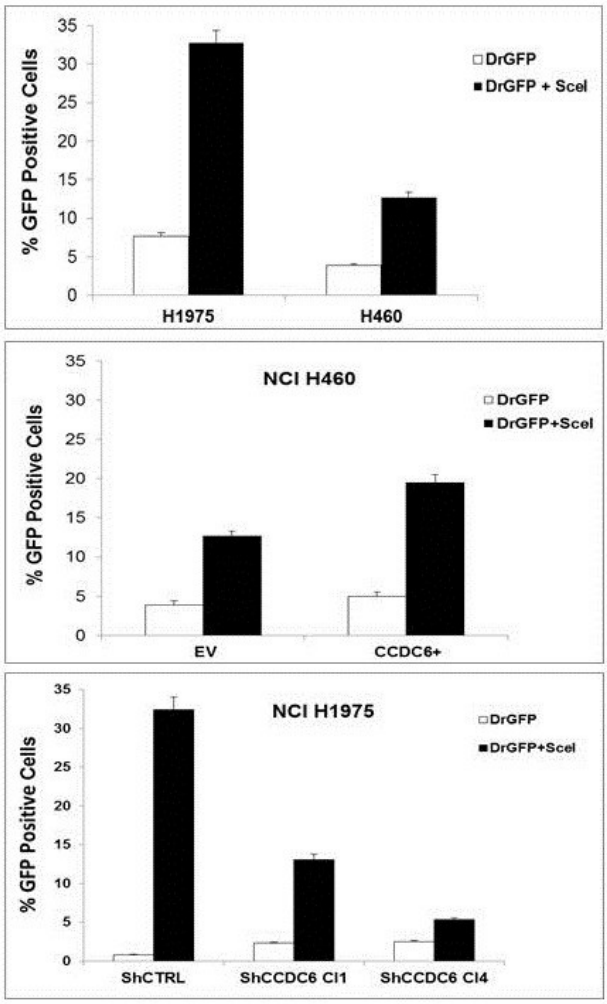

Fig. 16: CCDC6 loss affects HR in NSCLC cell lines

The myc-CCDC6 expression in H460 cells is shown (Figure 17).

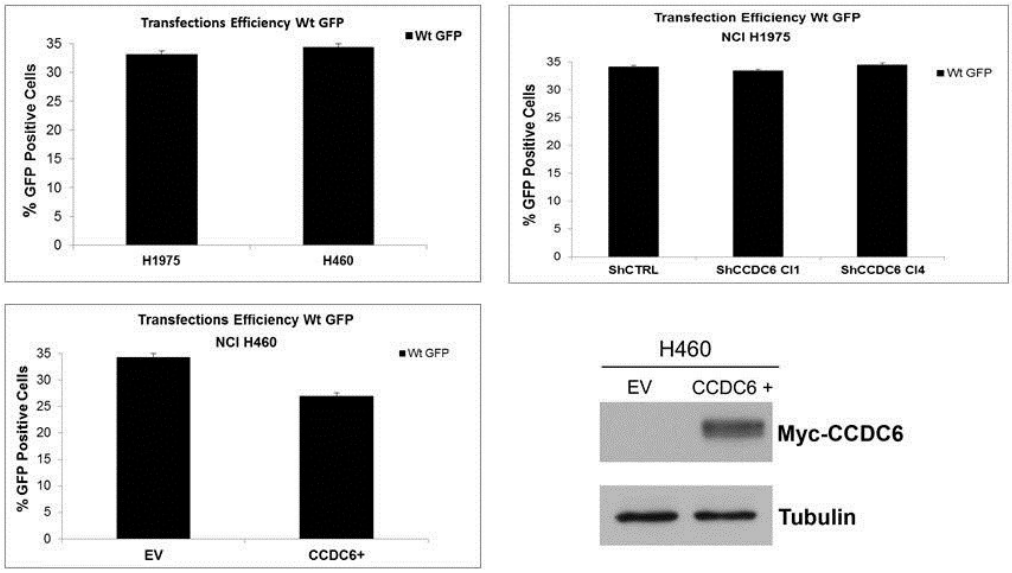

Fig. 17: Transfection efficiency of DR-GFP and I-SceI in NSCLC cell lines and myc-CCDC6 overexpression in H460 cells.

4.3 Platinum salts sensitivity in NSCLC H460 and H1975 cells

We hypothesized that low levels of CCDC6 in H460 cells could lead to the sensitivity to the PARP inhibitors, like in tumours leading alteration of key genes involved in Homologous-directed repair, such as BRCA1, also enhancing the sensitivity to the association of PARP-inhibitors with platinum salts.

We first assessed cellular toxicity for different concentration of cisplatinum in CCDC6 deficient and CCDC6 proficient lung cells by clonogenic survival assays. We observed that the CCDC6 deficient lung cancer cells, H460, were mostly resistant to platinum salts in all the ranges of the doses we utilized (Figure 18 top) compared to the NSCLC H1975 cells, CCDC6 proficient, that showed a high sensitivity at the same doses (Figure 18 bottom).

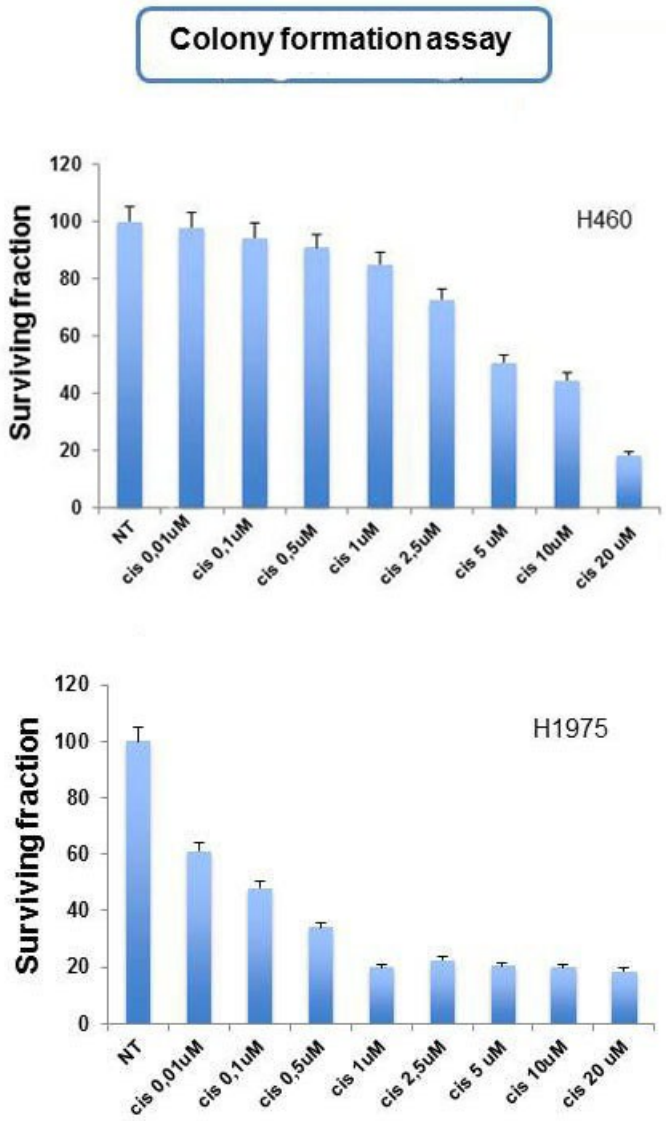

Fig. 18: Colony forming assay to evaluate the response to cisplatinum in H460 and H1975 NSC lung cancer cell lines.

We then hypothesized that low levels of CCDC6, combined to HR defects, could lead to the sensitivity to the PARP1/2 inhibitors, such as olaparib. To test this, we assessed the olaparib sensitivity in the H460 cells and also in the H1975 CCDC6 proficient NSCLC cell line, using the Cell Titer growth assay (Figure 19 and 22).

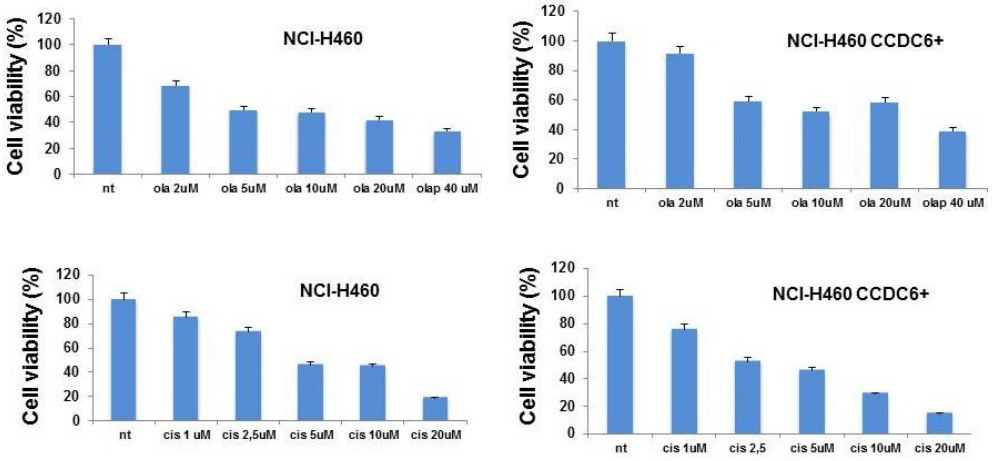

Fig. 19: Cell titer growth assay in NCI-H460 cells treated with different doses of olaparib or cisplatinum. The restoration of CCDC6 in H460 deficient cells recovered cisplatinum sensitivity and decreased sensitivity to olaparib.

Remarkably, no RET/PTC1 fusion or CCDC6 mutations have been reported in these cell lines (Matsubara D, 2012). We observed that in H460 NSC lung cancer cells the CCDC6 attenuation showed quite an elevated sensitivity to high doses of Olaparib, while a weak antiproliferative activity was evident at the lower doses of the Parp inhibitor drug (Figure 19 and 20).

By restoring CCDC6 expression in the H460 cells, we observed that the ectopic expression of CCDC6 significantly recovered cisplatinum sensitivity while decreasing sensitivity to olaparib (Figure 19 and 20).

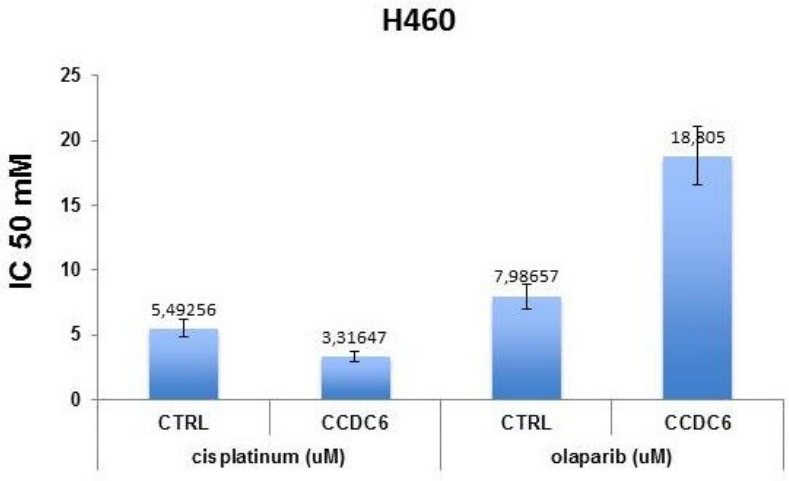

Fig. 20: IC50 values of cisplatinum and olaparib in H460 and H460CCDC6.

Next, H460 cells were treated with both the drugs in association, as we expected that the combination of cis-platinum with olaparib might show a synergistic effect in the CCDC6 deficient lung cancer cell lines.

The concentration ratio of Cisplatinum and Olaparib were designed to be molar ratios of 1:2. We observed an enhanced sensitivity to the drugs, when used in association. Olaparib specifically improved cis-platinum sensitivity on CCDC6 low H460 cells (Figure 21 bottom), as the combination of the two drugs showed a synergistic effect according to the CI in the H460 cells (Figure 21 top).

			cisplatinum + olaparib (uM)		
	cisplatinum (uM)	olaparib (uM)	*cis (uM)*	*ola (uM)*	C.I.
H460	5,10886	8,37244	1,03116	2,06233	0,44816

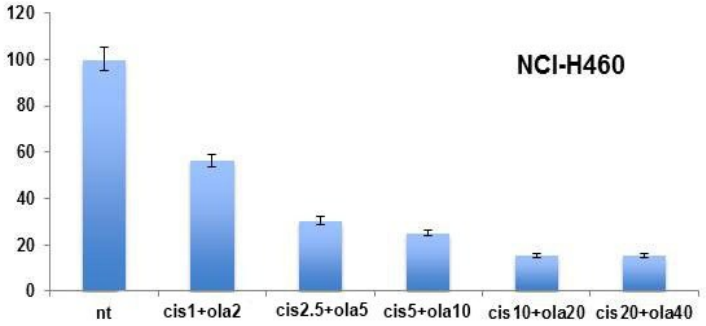

Fig. 21: Cisplatinum and Olaparib show synergism when utilized in association in H460.

Finally, to directly assess the relationship between CCDC6 deficiency and PARP1/2 inhibitor sensitivity, we stably silenced CCDC6 in the profoundly olaparib resistant H1975 NSC lung cancer cell line and assessed olaparib sensitivity (Figure 22 and 23).

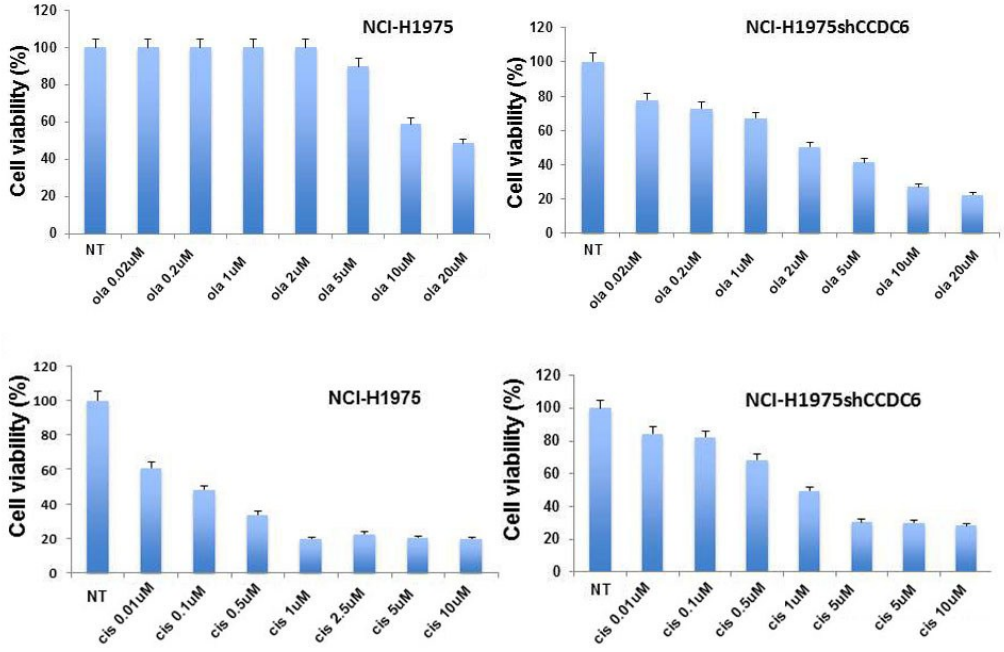

Fig. 22: Cell titer growth assay in NCI-H1975 cells, CCDC6 proficient, treated with different doses of olaparib or cisplatinum. The silencing of CCDC6 in H1975 decrease cisplatinum sensitivity and increase sensitivity to olaparib.

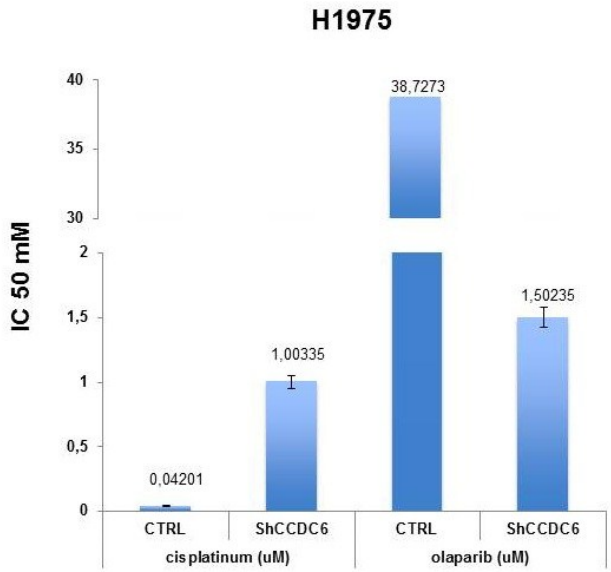

Fig. 23: IC50 values of cisplatinum and olaparib in H1975shCTRL and H1975shCCDC6.

Two different clones (H1975ShCCDC6 CL1 and CL4) were tested and a significant increase in olaparib sensitivity was achieved (data not shown). The ablation of CCDC6 in the NCI-H1975 cells (H1975shCCDC6 CL4) increased the sensitivity to olaparib (Figure 24 bottom) and the combination of olaparib with cisplatinum showed synergism (CI<1) (Figure 24 top).

			cisplatinum + olaparib		
	cisplatinum (μM)	olaparib (μM)	*cis (uM)*	*ola (uM)*	C.I.
H1975shCCDC6	1,00335	1,50235	0,25596	0,51193	0,59586

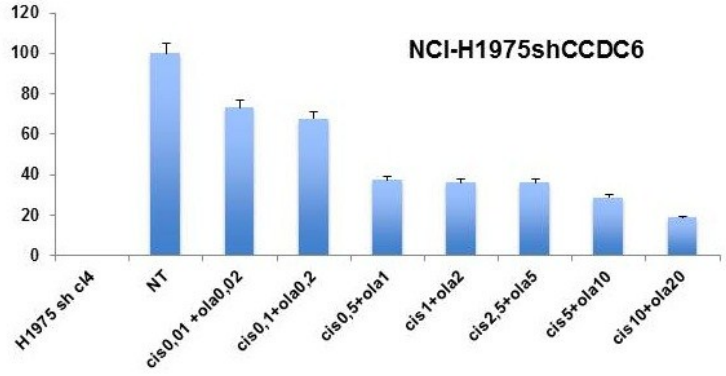

Fig. 24: Cisplatinum and Olaparib show synergism in H1975shCCDC6 when utilized in association.

4.4 CCDC6 expression in NSC lung tumors

For the purpose of assessing CCDC6 expression in a large series of human NSC lung tumour samples, we have analysed 138 primary tumours, at different stage, which underwent surgical tumour resection without any previous neoadjuvant treatment (Table 1).

Table 1. Characteristic of the patients			
Characteristc	**Patients with CCDC6 Low**	**Patients with CCDC6 High**	**All Patients (N=138)**
Pathologic TNM stage			
Stage IA	9 (29%)	22 (71%)	31 (100%)
Stage IB	20 (33.8%)	39 (66.2%)	59 (100%)
Stage IIA	1 (25%)	3 (75%)	4 (100%)
Stage IIB	8 (44.5%)	10 (55.5%)	18 (100%)
Stage IIIA	10 (62.5%)	6 (37.5%)	16 (100%)
Stage IIIB		4 (100%)	4 (100%)
Stage IV		1 (100%)	1 (100%)
Not Detected	3 (60%)	2 (40%)	5 (100%)
Tumour			
T1	10 (27.7%)	26 (72.3%)	36 (100%)
T2	33 (40.3%)	49 (59.7%)	82 (100%)
T3	4 (57%)	3 (43%)	7 (100%)
T4		4 (100%)	4 (100%)
Not Detected	4 (44.5%)	5 (55.5%)	9 (100%)
Lymph Node			
N+		5 (100%)	5 (100%)
N0	33 (31.4%)	72 (68.6%)	105 (100%)
N1	7 (63.6%)	4 (36.4%)	11 (100%)
N2	8 (72.7%)	3 (27.3%)	11 (100%)
NX		1 (100%)	1 (100%)
Not Detected	3 (60%)	2 (40%)	5 (100%)
Histologic Type			
ADC	23 (32.8%)	47 (67.2%)	70 (100%)
ASC	1 (100%)		1 (100%)
SCC	20 (42.5%)	27 (57.5%)	47 (100%)
Other	1 (10%)	9 (90%)	10 (100%)
Not Detected	6 (60%)	4 (40%)	10 (100%)

Table 2. N positivity distribution in different TNM stage

		Patients with CCDC6 Low	Patients with CCDC6 High	Grand Total
Low stage (IA-IIB)	N+	5 (41.7%)	7 (58.3%)	12 (100%)
	N0	33 (33%)	67 (67%)	100 (100%)
High stage (IIIA)	N+	10 (66.7%)	5 (33.3%)	15 (100%)
	N0		5 (100%)	5 (100%)
	Nx		1 (100%)	1 (100%)
Not Detected				5 (100%)

We performed the IHC analysis by taking advantage of the TMA technique that provides a great opportunity to easily analyze, store and share IHC data of all the selected patients. TMA immunostaining investigations of CCDC6 expression demonstrated that CCDC6 is barely detectable in about 30% of the NSCL tumours analyzed (45 out of 138).

Interestingly, the weak CCDC6 protein staining was significantly associated with the lymphonodal positivity ($p \leq 0,02$) (Table 2 and 3).

Table 3. Correlation between CCDC6 levels and lymph node positivity

CCDC6 low/high	**CCDC6**	**CCDC6**	
N	**Low**	**High**	**Grand Total**
N +	15 (57.7%)	11 (42.3%)	26 (100%)
N0	33 (31.4%)	72 (68.6%)	105 (100%)
Grand Total	48 (36.6%)	83 (63.4%)	13 (100%)

Student *t* Test **$p \leq 0.05$**

Moreover, we observed that this association was even stronger in the high stage group of tumours ($p \leq 0,01$) (Table 4), mainly represented by NSCLC of adenocarcinoma histotype.

Table 4. Correlation between CCDC6 levels and lymph node positivity in high stage

	High stage		
CCDC6 low/high N	**CCDC6 Low**	**CCDC6 High**	**Grand Total**
N +	10 (71.4%)	4 (28.6%)	14 (100%)
N0		5 (100%)	5 (100%)
Grand Total	10 (52.6%)	9 (47.4%)	19 (100%)
Chi square test		**p ≤ 0.05**	

Interestingly, a 10% occurrence of EGFR mutations was reported in a selected group of patients (7 out of 69). The EGFR mutations negatively correlated with the CCDC6 low staining phenotype (p ≤ 0,03 Fisher Exact Test) (Table 5).

Table 5. EGFR correlation with CCDC6 staining (Fisher's exact test)

Classification X	**EGFR status**
Classification Y	**CCDC6 low /high**

	Classification X		
Classification Y	MUT	WT	
HIGH	7	35	42 (60,9%)
LOW	0	27	27 (39,1%)
	7 (10,1%)	62 (89,9%)	69 (100%)

p = 0,03

Most importantly, a low CCDC6 staining was negatively correlated to the 60 months Disease Free Survival (DFS) and the Overall Survival rates for the NSCLC patients as shown by the Kaplan-Meier survival curves (Figure 25 and 26) (DFS *p ≤ 0.01*, and OS *p ≤ 0.05*, two-side log-rank test).

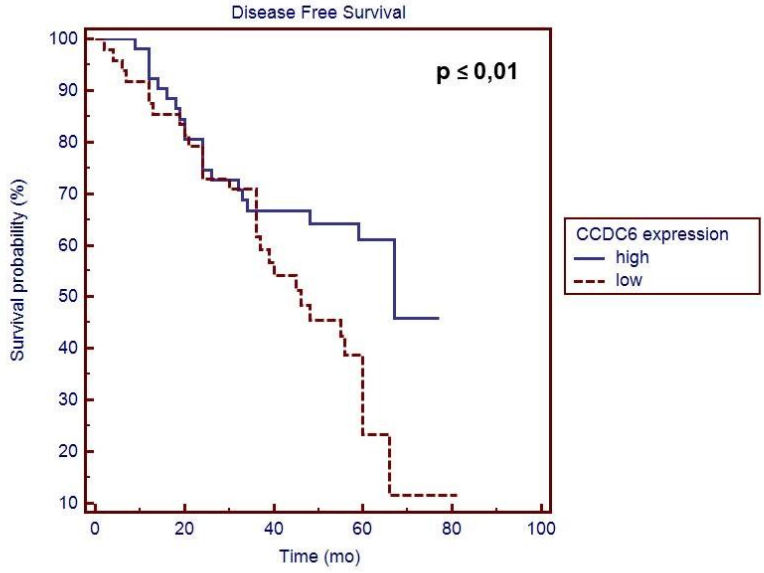

Fig. 25: Kaplan-Meier PDS plots, expressing disease free survival rate, for NSCLC patients grouped by the CCDC6 level of expression.

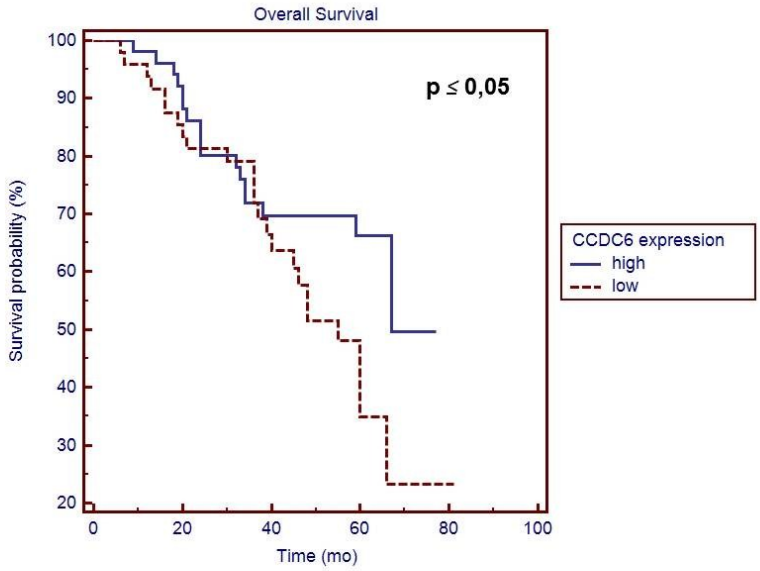

Fig. 26: Kaplan-Meier PDS plots, expressing overall survival rate, for NSCLC patients grouped by the CCDC6 level of expression.

Immunohistochemical stainings showing the analysis of whole sections of representative CCDC6 negative and positive samples are shown (Figure 27 and 28).

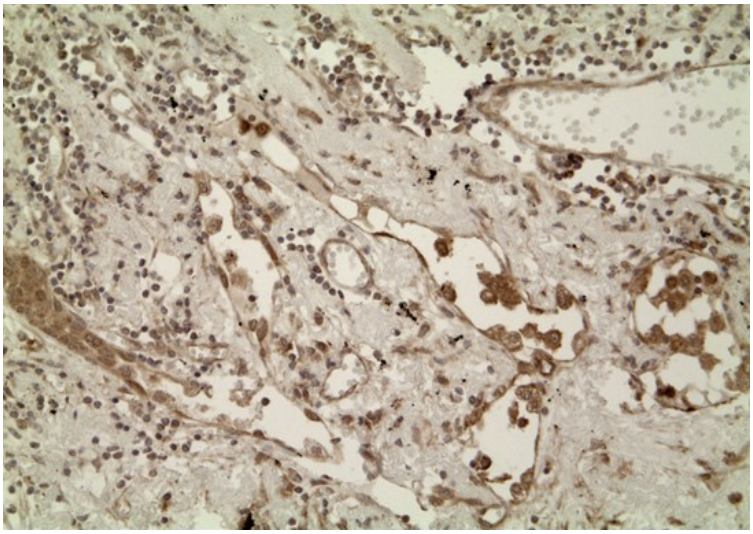

Fig. 27: CCDC6 IHC detection in NSCLC. The image is representative of CCDC6 low (0/+) **tumour** samples.

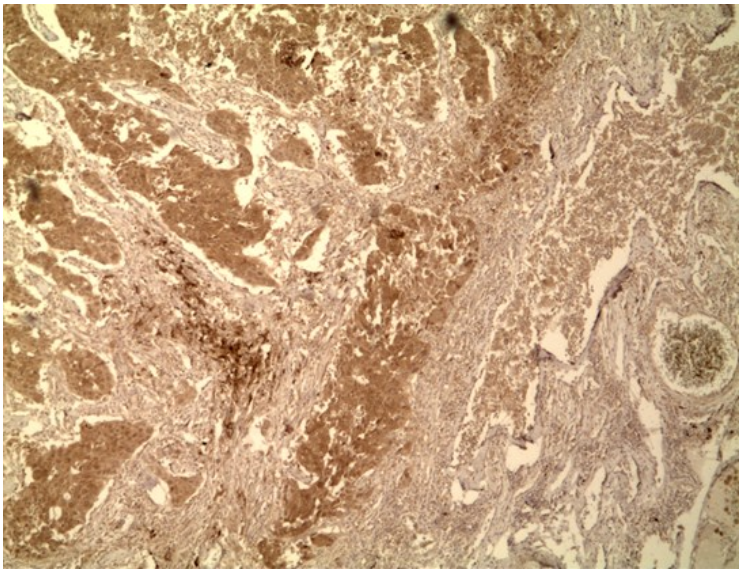

Fig. 28: CCDC6 IHC detection in NSCLC. The image is representative of CCDC6 high (+++) samples.

Finally, we analyzed CCDC6 mRNA levels in purified dissected cells from six representative NSCLC samples by RT-PCR; the mRNA analysis indicated that CCDC6 transcript levels did not show significant difference between the CCDC6-negative (Low) and CCDC6 positive (High) NSCLC representative samples suggesting that the different amount of the CCDC6 protein was mostly dependent on post-translational mechanisms (Figure 29).

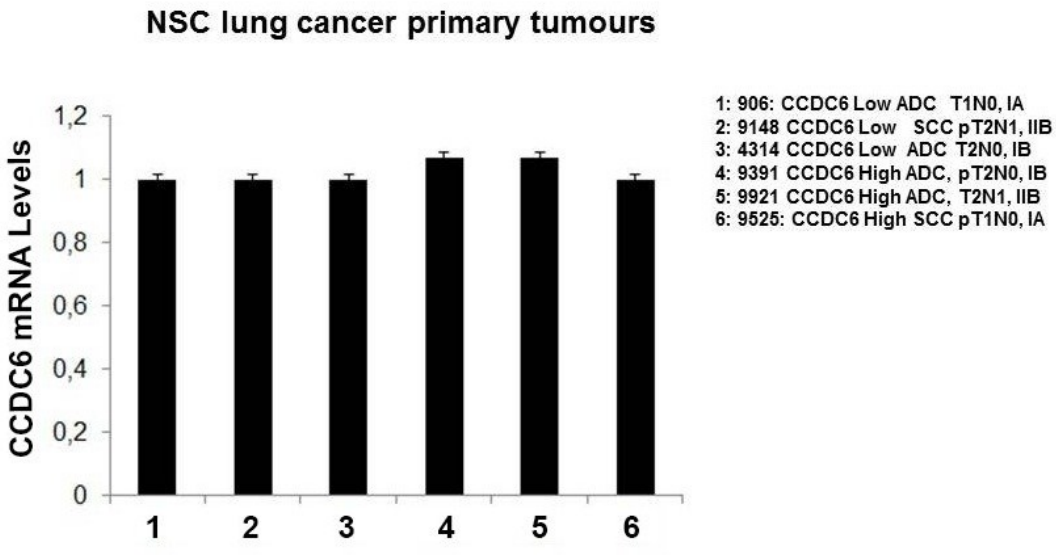

Fig. 29: CCDC6 mRNA expression in primary tumours.

CHAPTER 5–DISCUSSION AND CONCLUSIONS

Despite years of research and hundreds of reports on tumour markers in oncology, the number of those that have emerged as clinically useful is relatively restricted. Thus the assessment of new and reliable markers that can help clinicians to better diagnose human tumours and to predict the response to standard therapies and their outcome is of great relevance.

We here present some evidence suggesting that CCDC6 might be dowregulated on account of different genetic mechanisms affecting the repair of the damaged DNA and the sensitivity to different drugs, in human NSCLC.

The reasons which led us to choose NSCLC to study the CCDC6 expression levels include: (i) the occurrence of CCDC6 inactivation due to fusions with RET and the record of few CCDC6 somatic mutations in NSCLC (www.sanger.ac.uk/genetics/CGP/cosmic) (ii) the observation that, in the same tissue, CCDC6 is predicted as downregulated (by the analysis of the ArrayExpress Archive database), (iii) the high frequency of programmed DSBs as an essential part of genetic recombination during meiosis or in response to standard treatments in NSCLC and (iv) that CCDC6 depleted cells repair damaged DNA in a shorter time compared to controls (Merolla F et al, 2012).

In this study, we report the detection of a CCDC6 low staining at IHC in 30% of NSCLC, with no particular differences between adeno- and epidermoid carcinoma histotypes. The low intensity of CCDC6 staining significantly associates with aggressiveness, in a group of completely resected NSCLC patients (stage I – IIIA). Interestingly, in a selected group of patients (N = 69) we detected a 10% occurrence of EGFR mutations that negatively correlated with the CCDC6 low phenotype ($p \leq 0.03$) suggesting the mutual exclusivity of the two events.

Notably, the low CCDC6 expression negatively correlated with the disease free survival rate (log rank test $p \leq 0,01$) and the overall survival rate (log rank test $p \leq 0,05$). These results suggest that the inclusion of CCDC6 in NSCLC clinical studies should provide an additional prognostic marker for the overall survival.

Multivariate analyses to assess survival with respect to CCDC6 togheter with already validated biomarkers need to be performed, in

order to estimate the impact of these factors on overall survival and on disease free survival. Moreover, the data obtained by the in vitro cell lines treatment suggest that the low CCDC6 staining should have a predictive value for the resistance to conventional treatments in NSCLC patients. Therefore, retrospective analysis on archival samples of locally advanced tumours from treated patients who received chemio adjuvant therapy and perspective studies on diagnostic samples from elderly NSCLC patients with advanced metastatic disease are ongoing to the aim of evaluate the cisplatinum response with the objective to ameliorate the customized therapy in a near future.

The CCDC6 mRNA analysis of representative FFPE primary samples as well as the CCDC6 mRNA evaluation of NSCLC cell lines, which exhibit different CCDC6 protein levels, did not show any difference in terms of mRNA transcript levels. This suggests that the different amount of the CCDC6 protein, between different samples, was likely to be dependent on post-translational mechanisms on account of the activities of the CCDC6 modifier enzymes, which affect the CCDC6 protein stability and that are currently under investigation (Cerrato A et al, in preparation). These findings should also indicate novel therapeutic opportunities in NSCLC, in a near future.

We have recently reported that CCDC6 is important for the maintenance of the genome stability as its loss impairs the H2AX, Chk1 and RPA2 phosphorylation increasing a NHEJ-mediated repair, in response to genotoxic stress (Merolla F, 2012).

In CCDC6 lung deficient cells, Chk1 activation was attenuated after irradiation. Chk1 has a critical role in maintaining genome stability by delaying S- and G2-phase progression after DNA damage to allow time to the cells for repair before mitosis. Moreover, Chk1 depleted cells failed to form Rad51 nuclear foci after exposure to genotoxic stress, as reported.

Following IR exposure, in CCDC6 deficient NSC lung cancer cells we also observed a few gH2AX and Rad51 foci, associated to the impairment of HR evaluated by specific assays. The HR defects, caused by the CCDC6 deficiency, sensitized tumour cells to potent inhibitors of the DNA repair enzymes in vitro.

In fact, in the CCDC6 deficient H460 NSCLC tumourigenic cell line we observed an increase of sensitivity to olaparib and to the combination of olaparib with the platinum salts, that resulted in a synergistic effect (CI<1). These results suggested that CCDC6 might be

used as a biomarker of PARP1 inhibitor first line treatment. A few phase II trials that include PARP1 inhibitors are ongoing in NSCLC (www.cancer.gov/clinical trials) and in the near future it might be relevant to correlate the CCDC6 expression levels with the response to PARP1 inhibitors. The relevance of CCDC6 staining to predict resistance to cisplatinum salts should also be considered and extended to other tumours that are routinely treated with cisplatinum. As most of these tumours also carry DSB defects, on account of different sporadic genetic alterations, besides the BRCA1/2 germinal mutations, the relevance of the predictive value of CCDC6 to indicate sensitivity to the PARP inhibitors should also be taken into consideration.

Finally, we suggest that immunostaining quantification and the intracellular localization of CCDC6 in tumours could help to identify the more aggressive intratumoural clones, guiding therapeutic strategies and predicting tumours outcomes, as the intratumoural cell heterogeneity still represents a great challenge in terms of tumour aggressiveness and therapy resistance.

CHAPTER 6–ACKNOWLEDGEMENTS

At the end of my PhD course, I would like to express my gratitude to all the people who contributed with their continuous support to the realization of this dissertation after the three years of study and research.

First of all I would like to aknowledge Prof. Lucio Nitsch, co-ordinator of the International Doctorate in Genetics and Molecular Medicine, who has been continuously sustaining and supporting me, also in the critical moments.

I spent a brief but extremely focused and fruitful time in the laboratory of Prof. Mark T. Muller at the University of Central Florida (Orlando, USA) and I wish to thank him and all his co-workers for their kind hospitality.

I have word of thanks for Dr Angela Celetti who welcomed me in her group stimulating my scientific curiosity and offering me all her support and encouragement in order to conduct me to the end of my PhD doctoral course.

I need to thank “CREME Campania Research In Experimental Medicine” for the economic support in the year 2012-2013 in Italy and for the opportunity to spend a short term fellowship in USA, in Prof. Muller’s Lab.

I’m very grateful to all members of my laboratory at IEOS CNR for their collaborative spirit, for their friendly susteinance and for the great help in the daily work.

Finally my gratitude goes to my family for the lovely encouragement.

CHAPTER 7–REFERENCES

Bakkenist CJ, Kastan MB. DNA damage activates ATM through intermolecular autophosphorylation and dimer dissociation. Nature. 2003; 421(6922): 499-506.

Bartek J, Lukas J. Chk1 and Chk2 kinases in checkpoint control and cancer. Cancer Cell. 2003; 3(5): 421-9.

Beausoleil SA, Jedrychowski M, Schwartz D, Elias JE, Villén J, Li J, Cohn MA, Cantley LC, Gygi SP. Large-scale characterization of HeLa cell nuclear phosphoproteins. Proc Natl Acad Sci U S A. 2004; 101(33): 12130-5.

Brill LM, Salomon AR, Ficarro SB, Mukherji M, Stettler-Gill M, Peters EC. Robust phosphor - proteomic profiling of tyrosine phosphorylation sites from human T cells using immobilized metal affinity chromatography and tandem mass spectrometry. Anal Chem. 2004; 76(10): 2763-72.

Burma S, Chen BP, Murphy M, Kurimasa A, Chen DJ. ATM Phosphorylates Histone H2AX in Response to DNA Double-strand Breaks. J. Biol. Chem. 2001; 276:42462-42467.

Celetti A, Cerrato A, Merolla F, Vitagliano D, Vecchio G, Grieco M. H4(D10S170), a gene frequently rearranged with RET in papillary thyroid carcinomas: functional characterization. Oncogene. 2004; 23(1): 109-21.

Chang A. Chemotherapy, chemoresistance and the changing treatment landscape for NSCLC. Lung Cancer. 2011; 71(1): 3-10.

Chou TC and Talaly P. A simple generalize equation of multiple inhibition of Michealeis – Menten kinetic system. J. Biol. Chem. 1977, 252:6438-6442.

Drechsler M, Hildebrandt B, Kündgen A, Germing U, Royer-Pokora B. Fusion of H4/D10S170 to PDGFRbeta in a patient with chronic myelomonocytic leukemia and long-term responsiveness to imatinib. Ann Hematol 2007. 86(5): 353-4.

Dueva R, Iliakis G. Alternative pathways of non-homologous end joining (NHEJ) in genomic instability and cancer. Transl. Cancer Res. 2013; 2(3): 163-177.

Ewing RM, Chu P, Elisma F, Li H, Taylor P, Climie S, McBroom-Cerajewski L, Robinson MD, O'Connor L, Li M, Taylor R, Dharsee M, Ho Y, Heilbut A, Moore L, Zhang S, Ornatsky O, Bukhman YV, Ethier M, Sheng Y, Vasilescu J, Abu-Farha M, Lambert JP, Duewel HS, Stewart II, Kuehl B, Hogue K, Colwill K, Gladwish K, Muskat B, Kinach R, Adams SL, Moran MF, Morin GB, Topaloglou T, Figeys D. Large-scale mapping of human protein-protein interactions by mass spectrometry. Mol Syst Biol. 2007; 3:89.

Fernandez-Capetillo O, Lee A, Nussenzweig M, Nussenzweig A. H2AX: the histone guardian of the genome. DNA Repair 2004; 3(8-9): 959-67.

Fong PC, Yap TA, Boss DS, Carden CP, Mergui-Roelvink M, Gourley C, De Greve J, Lubinski J, Shanley S, Messiou C, A'Hern R, Tutt A, Ashworth A, Stone J, Carmichael J, Schellens JH, de Bono JS, Kaye SB. Poly(ADP)-ribose polymerase inhibition: frequent durable responses in BRCA carrier ovarian cancer correlating with platinum-free interval. J Clin Oncol. 2010; 28(15): 2512-19.

Freeman AK, Monteiro AN. Phosphatases in the cellular response to DNA damage. Cell Commun Signal. 2010; 8: 27.

Fusco A, Grieco M, Santoro M, Berlingieri MT, Pilotti SA, Pierotti MA, Della Porta G, Vecchio G. New oncogene in human thyroid papillary carcinomas and their lymph-nodal metastases. Nature.1987;328:170–2.

Gelmon KA, Tischkowitz M, Mackay H, Swenerton K, Robidoux A, Tonkin K, Hirte H, Huntsman D, Clemons M, Gilks B, Yerushalmi R, Macpherson E, Carmichael J, Oza A. Olaparib in patients with recurrent high-grade serous or poorly differentiated ovarian carcinoma or triple-negative breast cancer: a phase 2, multicentre, open-label, non-randomised study. Lancet Oncol. 2011; 12(9): 852-61.

Grieco M, Cerrato A, Santoro M, Fusco A, Melillo RM, Vecchio G. Cloning and characterization of H4 (D10S170), a gene involved in RET rearrangements in vivo. Oncogene. 1994; 9(9): 2531-5.

Grieco M, Santoro M, Berlingieri MT, Melillo RM, Donghi R, Bongarzone I, Pierotti MA, Della Porta G, Fusco A, Vecchio G. PTC is a novel

rearranged form of the ret proto-oncogene and is frequently detected in vivo in human thyroid papillary carcinomas. Cell. 1990;60:557–563.

Haber JE. Partners and pathways repairing a double-strand break. Trends Genet. 2000; 259–264.

Hoeijmakers JH. Genome maintenance mechanisms for preventing cancer. Nature. 2001; 411(6835): 366-74.

Jemal A, Siegel R, Ward E, Hao Y, Xu J, Murray T, Thun MJ. Cancer statistics, 2008. J Clin. 2008; 58(2): 71-96.

Jemal A, Siegel R, Ward E, Hao Y, Xu J, Thun MJ. Cancer Statistics, 2009. CA CANCER J Clin. 2009; 59: 225-249.

Jhiang SM. The RET proto-oncogene in human cancers. Oncogene 2000; 19(49): 5590-7.

Johnson JL, Pillai S, Chellappan SP. Genetic and biochemical alterations in non-small cell lung cancer. Biochem Res Int. 2012; 940405.

Kiyoshi Okamoto, Kotaro Kodama, Kazuma Takase, Naoko Hata Sugi, Yuji Yamamoto, Masao Iwata, Akihiko Tsuruoka. Antitumor activities of the targeted multi-tyrosine kinase inhibitor lenvatinib (E7080) against RET gene fusion-driven tumor models. Cancer Letters 2013; 97–103.

Kulkarni S, Heath C, Parker S, Chase A, Iqbal S, Pocock CF, Kaeda J, Cwynarski K, Goldman JM, Cross NC. Fusion of H4/D10S170 to the platelet-derived growth factor receptor beta in BCR-ABL-negative myeloproliferative disorders with a t(5;10)(q33;q21). Cancer Res. 2000; 60(13): 3592-8.

Kumagai A, Dunphy WG. Claspin, a novel protein required for the activation of Chk1 during a DNA replication checkpoint response in Xenopus egg extracts. Mol Cell. 2000; 6(4): 839-49.

Kummar S, Chen A, Parchment RE, Kinders RJ, Ji J, Tomaszewski JE, Doroshow JH. Advances in using PARP inhibitors to treat cancer. BMC Med. 2012; 10: 25.

Kummar S, Kinders R, Gutierrez ME, Rubinstein L, Parchment RE, Phillips LR, Ji J, Monks A, Low JA, Chen A, Murgo AJ, Collins J, Steinberg SM, Eliopoulos H, Giranda VL, Gordon G, Helman L, Wiltrout R, Tomaszewski JE, Doroshow JH. Phase 0 clinical trial of the poly

(ADP-ribose) polymerase inhibitor ABT-888 in patients with advanced malignancies. J Clin Oncol. 2009; 27(16): 2705-11.

Lee JH and Paull TT. Activation and regulation of ATM kinase activity in response to DNA double-strand breaks. Oncogene 2007; 7741–7748.

Leone V, Mansueto G, Pierantoni GM, Tornincasa M, Merolla F, Cerrato A, Santoro M, Grieco M, Scaloni A, Celetti A, Fusco A. CCDC6 represses CREB1 activity by recruiting histone deacetylase 1 and protein phosphatase 1. Oncogene. 2010; 29(30): 4341-51.

Lieber MR. The mechanism of human nonhomologous DNA end joining. J. Biol. Chem. 2008; 283; 1–5.

Loveday C, Turnbull C, Ramsay E, Hughes D, Ruark E, Frankum JR, Bowden G, Kalmyrzaev B, Warren-Perry M, Snape K, Miedzybrodzka Z, Morrison PJ, Paterson J, Porteous M, Rogers MT, Shanley S, Walker L, Ashworth A, Reis-Filho JS, Antoniou AC, Rahman N. Germline mutations in RAD51D confer susceptibility to ovarian cancer. Nature Genetics 2011 43, 879–882

Luise C, Merolla F, Leone V, Paladino S, Sarnataro D, Fusco A, Celetti A. Identification of sumoylation sites in CCDC6, the first identified RET partner gene in papillary thyroid carcinoma, uncovers a mode of regulating CCDC6 function on CREB1 transcriptional activity. PLoS One 2012; 7(11): e49298.

Lupas A, Van Dyke M, Stock J. Predicting coiled coils from protein sequences. Science. 1991; 252(5009): 1162-4.

Mao Z, Bozzella M, Seluanov A, Gorbunova V. Comparison of nonhomologous end joining and homologous recombination in human cells. DNA Repair 2008; 7(10): 1765-71.

Merolla F, Luise C, Muller MT, Pacelli R, Fusco A, Celetti A. Loss of CCDC6, the First Identified RET Partner Gene, Affects pH2AX S139 Levels and Accelerates Mitotic Entry upon DNA Damage. PLoS One 2012; 7(5): e36177.

Merolla F, Pentimalli F, Pacelli R, Vecchio G, Fusco A, Grieco M, Celetti A. Involvement of H4(D10S170) protein in ATM-dependent response to DNA damage. Oncogene. 2007;26(42):6167-75.

Minami D, Takigawa N, Takeda H, Takata M, Ochi N, Ichihara E, Hisamoto A, Hotta K, Tanimoto M, Kiura K. Synergistic effect of olaparib

with combination of cisplatin on PTEN-deficient lung cancer cells. Mol Cancer Res. 2013; 11(2): 140-8.

Minna JD, and Schiller,JH. Lung cancer. In Harrison Principles of Internal Medicine 17th Edition. 2008. pp. 551-562.

Mohammad DH, Yaffe MB. 14-3-3 proteins, FHA domains and BRCT domains in the DNA damage response. DNA Repair (Amst). 2009; 8(9): 1009-17.

Murai J, Huang SY, Das BB, Renaud A, Zhang Y, Doroshow JH, Ji J, Takeda S, Pommier Y. Trapping of PARP1 and PARP2 by Clinical PARP Inhibitors. Cancer Res. 2012; 72(21): 5588-99.

Nakada S, Chen GI, Gingras AC, Durocher D. PP4 is a gamma H2AX phosphatase required for recovery from the DNA damage checkpoint. EMBO Rep. 2008; 9(10):1019-26.

Okamoto K, Kodama K, Takase K, Sugi NH, Yamamoto Y, Iwata M, Tsuruoka A. Antitumor activities of the targeted multi-tyrosine kinase inhibitor lenvatinib (E7080) against RET gene fusion-driven tumor models. Cancer Lett. 2013; 340(1): 97-103.

Pao W, Hutchinson KE. Chipping away at the lung cancer genome. Nat Med. 2012; 18(3): 349-51.

Pierce AJ, Johnson RD, Thompson LH , Jasin M. XRCC3 promotes homology-directed repair of DNA damage in mammalian cells. Genes Dev. 1999; 13(20): 2633–2638.

Pierotti MA, Santoro M, Jenkins RB, Sozzi G, Bongarzone I, Grieco M, Monzini N, Miozzo M, Herrmann MA, Fusco A, Hay ID, Della Porta G, Vecchio G. Characterization of an inversion on the long arm of chromosome 10 juxtaposing D10S170 and RET and creating the oncogenic sequence RET/PTC. Proc Natl Acad Sci U S A. 1992; 89(5): 1616-20.

Postel-Vinay S, Bajrami I, Friboulet L, Elliott R, Fontebasso Y, Dorvault N, Olaussen KA, André F, Soria J-C, Lord CJ, Ashworth A. A high-throughput screen identifies PARP1/2 inhibitors as a potential therapy for ERCC1-deficient non-small cell lung cancer. Oncogene 2013; 32, 5377–5387.

Povlsen LK, Beli P, Wagner SA, Poulsen SL, Sylvestersen KB, Poulsen JW, Nielsen ML, Bekker-Jensen S, Mailand N, Choudhary C. Systems-wide analysis of ubiquitylation dynamics reveals a key role for PAF15 ubiquitylation in DNA-damage bypass. Nat Cell Biol. 2012; 14(10): 1089-98.

Puxeddu E, Knauf JA, Sartor MA, Mitsutake N, Smith EP, Medvedovic M, Tomlinson CR, Moretti S, Fagin JA. RET/PTC-induced gene expression in thyroid PCCL3 cells reveals early activation of genes involved in regulation of the immune response. Endocr Relat Cancer. 2005; 12(2): 319-34.

Rogakou EP, Pilch DR, Orr AH, Ivanova V, Bonner WM. DNA Double-stranded Breaks Induce Histone H2AX Phosphorylation on Serine 139. J. Biol. Chem. 1998; 273: 5858-5868.

San Filippo J, Sung P, Klein H. Mechanism of eukaryotic homologous recombination. Annual Rev. Biochem. 2008; 105: 16906-11.

Sandhu SK, Schelman WR, Wilding G, Moreno V, Baird RD, Miranda S, Hylands L, Riisnaes R, Forster M, Omlin A, Kreischer N, Thway K, Gevensleben H, Sun L, Loughney J, Chatterjee M, Toniatti C, Carpenter CL, Iannone R, Kaye SB, de Bono JS, Wenham RM. The poly(ADP-ribose) polymerase inhibitor niraparib (MK4827) in BRCA mutation carriers and patients with sporadic cancer: a phase 1 dose-escalation trial. Lancet Oncol. 2013; 14(9): 882-92.

Satoh MS, Poirier GG, Lindahl T. NAD'-dependent Repair of Damaged DNA by Human Cell Extracts. J Biol Chem. 1993; 268(8): 5480-7.

Schwaller J, Anastasiadou E, Cain D, Kutok J, Wojiski S, Williams IR, LaStarza R, Crescenzi B, Sternberg DW, Andreasson P, Schiavo R, Siena S, Mecucci C, Gilliland DG. H4(D10S170), a gene frequently rearranged in papillary thyroid carcinoma, is fused to the platelet-derived growth factor receptor beta gene in atypical chronic myeloid leukemia with t(5;10)(q33;q22). Blood. 15; 97(12): 3910-8.

Sonoda E Hochegger H, Saberi A, Taniguchi Y, Takeda S. Differential usage of non-homologous end-joining and homologous recombination in double strand break repair. DNA Repair 2006 8; 5(9-10): 1021-9.

Sos ML, Koker M, Weir BA, Heynck S, Rabinovsky R, Zander T, Seeger JM, Weiss J, Fischer F, Frommolt P, Michel K, Peifer M, Mermel C, Girard L, Peyton M, Gazdar AF, Minna JD, Garraway LA, Kashkar H,

Spiegel DR. PARP Inhibitors in Lung Cancer. Journal of Thoracic Oncology 2012; 7(16 Suppl 5): S392-3.

Staibano S, Ilardi G, Leone V, Luise C, Merolla F, Esposito F, Morra F, Siano M, Franco R, Fusco A, Chieffi P, Celetti A. Critical role of CCDC6 in the neoplastic growth of testicular germ cell tumors. BMC Cancer. 2013;13: 433.

Takeuchi K, Soda M, Togashi Y, Suzuki R, Sakata S, Hatano S, Asaka R, Hamanaka W, Ninomiya H, Uehara H, Lim Choi Y, Satoh Y, Okumura S, Nakagawa K, Mano H, Ishikawa Y. RET, ROS1 and ALK fusions in lung cancer. Nat Med. 2012;18(3):378-81.

Thun MJ, Hannan LM, Adams-Campbell LL, Boffetta P, Buring JE, Feskanich D, Flanders WD, Jee SH, Katanoda K, Kolonel LN, Lee IM, Marugame T, Palmer JR, Riboli E, Sobue T, Avila-Tang E, Wilkens LR, Samet JM. Lung cancer occurrence in never-smokers: an analysis of 13 cohorts and 22 cancer registry studies. PLoS Med. 2008; 5(9): e185.

Tong Q, Li Y, Smanik PA, Fithian LJ, Xing S, Mazzaferri EL, Jhiang SM. Characterization of the promoter region and oligomerization domain of H4 (D10S170), a gene frequently rearranged with the ret proto-oncogene. Oncogene 1995; 10(9): 1781-7.

Tong Q, Xing S, Jhiang SM. Leucine zipper-mediated dimerization is essential for the PTC1 oncogenic activity. J Biol Chem. 1997; 272(14): 9043-7.

Tutt A, Bertwistle D, Valentine J, Gabriel A, Swift S, Ross G, Griffin C, Thacker J, Ashworth A. Mutation in Brca2 stimulates error-prone homology-directed repair of DNA double-strand breaks occurring between repeated sequences. EMBO J. 2001; 20(17): 4704–4716.

Walker S. Updates in non-small cell lung cancer. Clin J Oncol Nurs. 2008; 12(4): 587-96.

Ye Y, Wang D, Su C, Rong T, Guo A. Combined detection of p53, p16, Rb, and EGFR mutations in lung cancer by suspension microarray. Genet Mol Res. 2009; 8(4): 1509-18.

Zhao J, Tang J, Men W, Ren K. FBXW7-mediated degradation of CCDC6 is impaired by ATM during DNA damage response in lung cancer cells. FEBS Lett. 2012; 586(24): 4257-63.

Zhou BB, Elledge SJ. The DNA damage response: putting checkpoints in perspective. Nature. 2000; 408(6811): 433-9.